# A Forebrain Hub for Cautious Actions via the Midbrain

Ji Zhou*, Muhammad S. Sajid*, Sebastian Hormigo, and Manuel A. Castro-Alamancos

Department of Neuroscience
University of Connecticut School of Medicine
Farmington CT 06030-3401 USA

* Equal contribution

Correspondence: Manuel Castro-Alamancos, PhD
Department of Neuroscience
University of Connecticut School of Medicine
263 Farmington Avenue
Farmington, CT 06030-3401 USA
Email: mcastro@uchc.edu

Number of Figures: 14

**Abbreviated title:** STN and goal-directed action timing

**Acknowledgments:** Supported by NIH grants to MAC. We thank Mariana Mangini for technical assistance.

## Abstract

Adaptive goal-directed behavior requires dynamic coordination of movement, motivation, and environmental cues. Among these, cautious actions, where animals adjust their behavior in anticipation of predictable threats, are essential for survival. Yet, their underlying neural mechanisms remain less well understood than those of appetitive behaviors. Using calcium imaging in freely moving mice, we show that glutamatergic neurons in the subthalamic nucleus (STN) are robustly engaged during cue-evoked avoidance and exploratory behavior, encoding both contraversive movement and cautious responding. Targeted lesions and optogenetic manipulations reveal that STN projections to the midbrain, but not to the globus pallidus, are necessary for executing cued avoidance. Moreover, the frequency of STN activation governs response timing, accelerating the initiation of goal-directed actions to the point that it becomes incompatible with passive response, without being aversive. These findings identify a critical role for the STN in orchestrating adaptive goal-directed behavior by directing timely actions via its midbrain projections.

**Significance statement**: This study provides new insights into the neural pathways that mediate adaptive goal-directed behaviors in response to environmental cues, identifying a critical role for glutamatergic projections from the subthalamic nucleus (STN) to the midbrain. We show that STN activation is essential for cued goal-directed actions, but high levels of activation are incompatible with cautious responding and passive actions where movement should be postponed or not initiated. These findings deepen our understanding of the circuits involved in cued goal-directed adaptive behaviors used to cope with contextual challenges, which are often altered by brain disorders.

## Introduction

Adaptive behavior often requires animals to take goal-directed actions in response to environmental cues that predict rewards or potential threats (Thorndike, 1898). The ability to initiate a response rapidly enough to prevent harm—yet not so prematurely that it leads to unnecessary risk—defines cautious behavior (e.g., vacillating before crossing the street). This form of behavioral control has been extensively studied through speed-accuracy trade-off tasks and evidence accumulation models, yet much of this work has focused on appetitive outcomes—such as the presentation or omission of reward— rather than the prospect of harmful, aversive consequences (Smith and Ratcliff, 2004; Gold and Shadlen, 2007; Bogacz et al., 2010; van Maanen et al., 2011; Guitart-Masip et al., 2012; Heitz and Schall, 2012; Ratcliff and Frank, 2012; Yee et al., 2022; Zhou et al., 2022). Understanding how the brain coordinates cautious decision-making under threat is critical for uncovering the neural mechanisms that guide adaptive, motivated actions.

The STN, located within the subthalamus alongside the GABAergic zona incerta, is primarily composed of glutamatergic neurons. It is a key component of the basal ganglia's indirect pathway, interconnecting with the globus pallidus externa (GPe) and projecting to the basal ganglia output nuclei, including the substantia nigra pars reticulata (SNr) in the midbrain. The STN integrates a diverse array of inputs from both forebrain and midbrain regions and provides a hyperdirect pathway from the cortex to the midbrain, bypassing the striatum (Kita and Kitai, 1987; Albin et al., 1989; Canteras et al., 1990; DeLong, 1990; Gerfen and Wilson, 1996; Smith et al., 1998; Nambu et al., 2002; Kita and Kita, 2011; Wilson and Bevan, 2011; Prasad and Wallen-Mackenzie, 2024). The role of the STN in self-paced movement and action control is well-documented (Isoda and Hikosaka, 2008; Bonnevie and Zaghloul, 2018; Klaus et al., 2019),

and it is a common deep brain stimulation (DBS) target for treating Parkinson's disease (Limousin et al., 1995; Gittis and Sillitoe, 2024). It is also targeted for treating obsessive compulsive disorder (OCD), which is characterized by abnormal, repetitive actions often triggered by external cues that the subject cannot inhibit (Mallet et al., 2008; Haber et al., 2021). However, there are divergent perspectives on STN's function during movement and action generation. Intriguingly, studies in humans suggest that STN is involved in action slowing or cautiousness in the face of conflict or difficulty (Frank et al., 2007; Cavanagh et al., 2014; Herz et al., 2024). It has also been implicated in action cancellation (Aron, 2011; Schmidt et al., 2013), although other studies propose that different pathways may mediate the stopping of actions (Mallet et al., 2016; Aristieta et al., 2021; Bevan, 2021; Friedman and Yin, 2023). Similarly, the involvement of STN in movement control is ambiguous; some studies report that STN activation suppresses movement (Fife et al., 2017; Guillaumin et al., 2021; Xie et al., 2022), while others indicate that it facilitates movement (Watson et al., 2021; Fan et al., 2023; Friedman and Yin, 2023). Moreover, recent recordings from STN neurons in head-fixed mice show activation correlated with self-paced locomotion (Callahan et al., 2024), but its activation during cued goal-directed actions where freely moving mice must generate slow onset, cautious responses in adaptive contexts has been less explored.

We recorded and manipulated STN neuron activity in freely behaving mice using cell-type-specific fiber photometry, miniscope calcium imaging, optogenetics, and genetically targeted lesions to investigate their role in exploratory and goal-directed behaviors. Our findings reveal that STN neurons encode contraversive movements and cautious, cued goal-directed avoidance actions characterized by slow onsets and are essential for generating them.

## Results

### *STN activity encodes movement in the contraversive direction*

To assess the population activity of glutamatergic STN neurons during movement, we expressed GCaMP7f (Chen et al., 2013) in these neurons by locally injecting a Cre-AAV in Vglut2-Cre mice (n=8). After implanting a single optical fiber within the STN, we employed calcium imaging fiber photometry, as previously described (Hormigo et al., 2021b; Hormigo et al., 2023; Zhou et al., 2023). Figure 1A illustrates a representative trajectory of the optical fiber targeting GCaMP-expressing glutamatergic STN neurons. The estimated imaged volume extends ~200 µm from the optical fiber ending, encompassing ~$2.5x10^7$ $\mu m^3$ (Pisanello et al., 2019).

In freely moving mice, we conducted continuous measurements of calcium fluorescence ($F/F_o$) and spontaneous movement while mice explored an arena. Cross-correlations were computed between movement and STN activation, to relate these continuous variables (Fig. 1B upper). Overall movement was strongly correlated with STN neuron activation. When the movement was dissociated into rotational and translational components, the cross-correlation predominantly involved the translational movement. A linear fit between the movement and $F/F_o$ (integrating over a 200 ms window), revealed a strong linear positive correlation between the STN activation and translational or rotational movement (Fig. 1B lower). These relationships were absent when one variable in the pair was shuffled (Fig. 1B, lower).

To further evaluate the relationship between movement and STN activation, we detected spontaneous movements and time extracted the continuous variables around the detected movements peaks (Fig. 1C) following the same procedures we used in other brain regions (Hormigo et al., 2023; Zhou et al., 2023). The detected movements were classified in three categories. The first category includes all peaks (Fig. 1C black traces), which revealed a strong

STN neuron activation in relation to movement. The second category includes movements that had no detected peaks 3 sec prior (Fig. 1C red traces), which essentially extracts movement onsets from immobility. This revealed a sharp activation in association with movement onset. The third category sampled the peaks by averaging every >5 seconds to eliminate from the average the effect of closely occurring peaks (Fig. 1C cyan traces). This category includes movement increases from ongoing baseline movement (instead of movement onsets from immobility) and showed a strong activation of STN neurons. For the three categories of movement peaks, the STN activation around movement was significant compared to baseline activity (Tukey $p<0.0001$). Thus, STN neurons discharge in relation to the occurrence of movement.

We next determined if the STN activation during movement depends on the direction of the head movement in the ipsiversive or contraversive direction. Figure 2A shows movement turns in the contraversive (Fig. 2A cyan) and ipsiversive (Fig 2A red) directions versus the recorded STN neurons. While the detected turns were opposite in direction and similar in amplitude, the STN neuron activation was sharper when the head turned in the contraversive direction. We compared the area, peak amplitude, and peak timing of the F/Fo activation between ipsiversive and contraversive turns. For *all turns* and *no turns 3 sec prior*, the F/Fo amplitude of contraversive turns was larger (Tukey $t(240)= 17.6$ $p<0.0001$ and Tukey $t(240)= 5.4$ $p=0.0001$) and peaked earlier (Tukey $t(240)= 3.22$ $p=0.02$ and Tukey $t(240)= 3.06$ $p=0.03$), while the area did not differ (Fig. 2B). The results were similar for *1 turn per >5 sec* but this category showed a stronger contrast between the peaks in both directions, resulting in a significant difference in both the area (Tukey $t(240)= 4.27$ $p=0.002$) and peak amplitude (Tukey $t(240)= 10.4$ $p<0.0001$) but not the peak timing, which becomes more variable for small peaks.

Therefore, STN glutamatergic neurons code movement direction discharging sharply to contraversive turns.

The preceding experiments involved calcium imaging fiber photometry, which integrates the activity of populations of STN glutamatergic neurons. Next, we employed miniscope calcium imagining recordings of individual STN glutamatergic neurons in freely behaving mice (n=5). In these mice, we expressed GCaMP7f by locally injecting a Cre-AAV in the STN of Vglut2-Cre mice and implanted a GRIN lens into the STN (Fig. 3A). We recorded the activity of STN neurons (1030 cells) as mice moved in a cage. The neurons were then classified according to their activation during spontaneous movements and orienting turns.

First, we recorded the F/F activity of individual neurons and identified movement onsets by detecting movements with no turns 3 seconds prior. The F/F time-series activity of each neuron around these movement onsets was extracted and classified using k-means clustering, revealing three distinct neuron classes. Fig. 3B illustrates the activation patterns of these classes. Class 1 neurons, comprising 56.5% of the neurons, showed minimal activation during movement onset. Class 2 neurons, representing 15.9% of the neurons, were inhibited as movement slowed before onset but did not exhibit sharp activation at onset, suggesting a slight modulation by movement speed. Class 3 neurons, accounting for 27.6% of the neurons, showed a sharp activation in relation to movement onset.

Second, we identified movement turns and extracted the F/F time-series activity of each neuron around ipsiversive and contraversive turns. The activity difference for each neuron was calculated per session to obtain a directional activation bias, which was classified using k-means clustering into three neuron classes. Figure 3C depicts the activation of these classes during ipsiversive and contraversive turns (middle and right panels), along with the directional

activation bias (left panel) used for classification. Figure 3D (top) shows the first two principal components from the k-means for all the cells. An equivalence test showed no significant difference in turn angles and movement amplitudes across the three classes ($F(2,1030) = 0.66$, $p = 0.55$). However, the peak F/F bias amplitudes during turns differed significantly between the classes (Fig. 3D bottom; $F(2,1030) = 1086.8$, $p < 0.0001$). Class 3 neurons (n = 192, 18.6%) exhibited a strong discharge to contraversive movements, significantly stronger than the other classes (Tukey $q > 30$, $p < 0.0001$ for Class 3 vs. Class 2 or Class 1). Class 2 neurons (n = 256, 24.8%) showed greater activation in the ipsiversive direction, but with a much weaker bias compared to Class 3. Class 1 neurons (n = 585, 56.6%) displayed minimal activation during turns. Thus, approximately 20% of STN neurons were strongly active during contraversive movements, while about 25% exhibited a weak bias towards ipsiversive movements.

***STN excitation drives movements in the ipsiversive direction***

Given that STN neurons encode more strongly contraversive movement direction, we hypothesized that exciting these neurons would elicit contraversive movements. To test this, we excited glutamatergic STN neurons by expressing ChR2 in the STN of Vglut2-Cre mice using bilateral injections of a Cre-inducible AAV and implanted a dual optical fiber bilaterally (STN-ChR2 mice, n = 11 mice). During open-field exploration, we applied blue light trains (1-ms pulses at 10, 20, 40, and 66 Hz for 2 seconds) to excite STN neurons unilaterally or bilaterally at varying levels. Light trains were delivered randomly at different intervals within the same sessions. These procedures were also performed in No Opsin control mice (n = 6), which did not express ChR2.

Unilateral optogenetic excitation of STN neurons produced a robust ipsiversive head orienting direction bias, with the strength of the effect depending on the frequency of blue light stimulation (Fig. 3E). Even the lowest effective stimulation frequencies and powers elicited ipsiversive movements. There was a significant effect of light frequency on directional bias in the STN-ChR2 mice (Fig. 3E; Mixed ANOVA Tukey $t(60)=8.6$ $p<0.0001$, 10-20 Hz vs 40-66 Hz) but not in the NoOpsin mice (Tukey $t(60)=0.7$ $p=0.94$). There was also a significant difference in directional bias between STN-ChR2 and No Opsin mice for 10-20 Hz (Fig. 3E; Tukey $t(60)=4.6$ $p=0.009$) and 40-66 Hz (Tukey $t(60)=11.3$ $p<0.0001$) blue light.

The effects of bilateral optogenetic excitation are further examined below; however, when compared directly within the STN-ChR2 group in the open field arena, bilateral stimulation induced significantly more movement than unilateral stimulation at both 10–20 Hz (2Way ANOVA Tukey $t(37)=3.3$ $p=0.02$ Unilateral vs Bilateral) and 40-66 Hz (Tukey $t(37)=8.4$ $p<0.0001$). The higher frequencies caused more movement than the lower frequencies when applied either unilaterally (Tukey $t(37)=7.3$ $p<0.0001$) or bilaterally (Tukey $t(37)=12.3$ $p<0.0001$).

Together, these findings indicate that STN excitation promotes movement in a frequency-dependent manner. However, the ipsiversive movements elicited by unilateral stimulation (Fig. 3E) stand in contrast to the contraversive direction encoded by STN neurons during spontaneous behavior (Fig. 3A–D). This dissociation suggests that while STN neurons encode contraversive movements, they may not directly drive them, highlighting a more complex role in movement modulation.

***STN neurons activate during goal-directed avoidance movement***

The results indicate that STN neurons activate during contraversive movement. Therefore, during fiber photometry recordings, we examined STN neuron activation across a series of cued (signaled) avoidance procedures (AA1, AA2, AA3, and AA4 (Zhou et al., 2022; Zhou et al., 2023) where mice either move (actively avoid) or withhold movement (passively avoid) to prevent an aversive US. These cued active and passive avoidance behaviors represent adaptive, goal-directed actions driven by their consequences, which mice learn rapidly and reliably.

Since these procedures are signaled by tones, we first conducted auditory mapping sessions to test if auditory tones activated STN neurons in freely behaving mice. During auditory mapping sessions (52 sessions in 6 mice; Fig. 4A,B), mice were placed in a small cage (half the size of a shuttle box) and 10 auditory tones of different saliencies, defined by sound pressure level (SPL in dB; low and high, ~70 and ~85 dB) and frequency (4, 6, 8, 12, 16 kHz), were presented in random order (1 sec tones every 4-5 sec, each repeated 10 times per session). The calcium signal evoked in STN neurons by the tones (0-1.5 sec window) depended on SPL (TwoWayRMAnova $F(1,51)= 22.85$ $p<0.0001$) and frequency ($F(4,204)= 5.3$ $p=0.0004$), but not their interaction ($F(4,204)= 0.9$ $p=0.45$). In general, higher SPL and frequency tones produced stronger STN activation (Fig. 4). However, these same effects were observed on movement (overall speed). Thus, the movement evoked by the tones also depended on tone SPL ($F(1,51)= 78.3$ $p<0.0001$) and frequency ($F(4,204)= 12.56$ $p<0.0001$), but not their interaction ($F(4,204)= 1.8$ $p=0.12$). The movement evoked by the tones consisted of both rotational and translational components (Fig. 4B), and each of these components showed the same effects as overall movement (SPL or frequency $p<0.0001$, interaction $p>0.07$). However, it is worth noting that the

amplitudes of F/Fo activation (0.1-0.2 zScore) and movements (~2-4 cm/sec) evoked by the tones are relatively small. The results indicate that STN neurons respond to salient auditory tones in association with movement.

We then measured STN neuron activation as the mice performed the avoidance procedures in a shuttle box (Fig. 5A). Figure 5B shows the behavioral performance of the animals in these tasks including the percentage of avoids (closed black circles), the avoid latencies (closed orange triangles), and the number of intertrial crossings (cyan bars). As previously shown, animals perform a large percentage of active avoids during the AA1, AA2, AA3-CS1, and AA4 procedures (Hormigo et al., 2021b). During AA2, ITCs are punished. Consequently, avoid latencies shift longer in an apparent reflection of caution (Zhou et al., 2022). During AA3, animals learn to discriminate between two CS's, passively avoiding when AA3-CS2 is presented. During AA4, the avoid latencies adapt to the varying duration of three active avoid intervals (4, 7, and 15 sec) signaled by different CS tones.

Figure 5C shows F/Fo and movement traces from CS onset for the AA1 (black), AA2 (red), and AA3 (green) avoidance procedures classified as correct responses (left panel, avoids; for AA3-CS2 correct passive avoids are shown in blue) or errors (right panel, escapes). During the avoidance procedures, the CS that drives active avoids (Fig. 5C black, red, green) caused a sharp and fast (<0.5 sec) F/Fo peak at CS onset, which is associated with the typical orienting head movement evoked by the CS depending on task contingencies and SPL (Zhou et al., 2023). Notably, AA3-CS2, which drives passive avoids, also produced a sharp STN activation at CS2 onset, even though it is associated with nil orienting head movement due to lower SPL. The STN activation evoked by CS2 tended to be smaller than the activation evoked by CS1 (2WayRMAnova $F(1,8)=5.05$ $p=0.05$ Factor1 CS1 vs CS2). Moreover, compared to correct

responses, errors (escapes to CS1 and active avoids to CS2) were associated with larger orienting response movements ($F(1,8)=7.4$ $p=0.02$ Factor2 Correct vs Error) and STN activation ($F(1,8)=8.6$ $p=0.01$). Thus, CS2 evoked an orienting STN activation not associated with movement, which may serve to prepare STN for the upcoming decision (active vs passive action). However, strong CS-evoked orienting movements (Zhou et al., 2023) and STN activation are associated with wrong decisions (errors), suggesting that an appropriate orienting movement and STN activation level are important for correct decisions about the CS signal.

The succeeding avoidance movement was associated with strong STN neuron activation (Fig. 5C avoids). In AA1, there was a large F/Fo peak related to the avoidance movement. As mice transitioned to AA2, the STN activation shifted to the right following the delayed avoid latencies characteristic of this procedure (Fig. 5C black vs red traces). Thus, the activation of STN neurons is closely associated with the active avoid movement. In addition, when mice failed to avoid, STN neurons activated very sharply in association with the fast escape responses evoked by the US during the escape interval (Fig. 5C escapes). Furthermore, during the AA3 procedure, only CS1, which drives active avoids, produced strong STN activation (Fig. 5C green). CS2, which drives passive avoids, produced little STN activation after the initial sharp peak caused by CS2 onset (Fig. 5C blue). To measure avoid and escape responses, we extracted the F/Fo and speed from the response occurrence for AA1, AA2, and AA3 (Fig. 5D). Both avoids and escapes were associated with robust STN activation during the three procedures (Fig. 5D,E). However, since escapes occurred at higher speeds (Tukey $t(5)= 9.85$ $p=0.0009$ avoids vs escapes), they were associated with stronger STN activation than avoids (Tukey $t(5)= 6.03$ $p=0.008$). Moreover, as is typical (Zhou et al., 2022), the speed of avoids was higher during AA2

compared to AA1 (Tukey $t(40)= 7.4$ $p<0.0001$ AA1 vs AA2), which tended to be reflected in a larger STN activation during AA2 (Tukey $t(40)= 3.4$ $p=0.05$).

During AA4, mice adapt their avoidance movement to the duration of the avoidance interval signaled by each of the three CSs (Hormigo et al., 2021b). Accordingly, STN activation shifted to reflect the avoidance movement (Fig. 6A). When responses were measured from response occurrence (Fig. 6A right panel and 6B), the CS1 avoids speed was faster than CS2 (Tukey $t(62)= 6.01$ $p=0.0002$) or CS3 (Tukey $t(62)= 8.85$ $p<0.0001$), consistent with the more imminent threat signaled by CS1, which has a shorter 4-sec avoidance interval. However, this was not reflected in a difference of the peak activation of STN neurons (RMAnova $F(2,62)= 1$ $p=0.37$).

Since mice have high rates of avoids in these tasks, and consequently relatively few escapes, we conducted additional sessions (Fig. 6C,D; 7 mice) in which the US (foot-shock and white noise) was presented unsignaled to drive an escape on every trial. To distinguish the contribution of the foot-shock and white noise presented by the US, additional trials in the same session presented the foot-shock or the white noise alone. The unsignaled US evoked a strong STN activation in association with the fast escapes. Presentation of the foot-shock alone produced STN activation and escapes like the full US. However, presentation of the white noise alone drove escapes at lower speeds, which were associated with less STN activation than the foot-shock alone (Tukey $t(10)= 4.4$ $p=0.02$ speed; Tukey $t(10)= 4.96$ $p=0.001$ F/Fo) or the full US (Tukey $t(10)= 5.3$ $p=0.09$ speed; Tukey $t(10)= 4.67$ $p=0.002$ F/Fo). Thus, the STN activation during unsignaled US presentations follows the speed of the escape movement driven by the stimuli. The auditory white noise component adds little to the foot-shock driven movement and STN activation.

In conclusion, STN neurons activate at CS onset even in the absence of overt orienting movement and then discharge more robustly during the ensuing active avoid and escape movements. STN activation is ideally suited to drive active avoids.

***STN neurons encode more robustly cautious actions***

We used miniscopes to image activity from individual STN neurons while mice performed signaled active avoidance. To characterize behavioral variability, we applied k-means clustering to the time series of movement speed following CS onset across avoidance trials (AA1/2). This analysis identified three distinct classes of avoidance responses (Fig. 7A, bottom gray panel). Class 1 responses (black) were marked by rapid avoidance movements initiated immediately after the orienting movement at CS onset. In contrast, Class 2 (red) and Class 3 (cyan) responses were initiated later, reflecting more cautious behavior (Zhou et al., 2022).

Class 2 and Class 3 avoidance responses differed from each other and from Class 1 in several behavioral features. First, baseline movement prior to CS onset (Fig. 7F, left panel) was lowest in Class 3 avoids compared to both Class 2 (Tukey $q = 5.85$, $p = 0.0001$) and Class 1 (Tukey $q = 18.12$, $p < 0.0001$), with Class 2 exhibiting the highest spontaneous movement. Second, the amplitude of the CS-evoked orienting response (Fig. 7F, 2nd panel from left) was significantly reduced in Class 3 avoids relative to Class 2 (Tukey $q = 9.77$, $p < 0.001$) and Class 1 (Tukey $q = 20.85$, $p < 0.0001$). Finally, the change in speed during the avoidance interval—measured as the baseline-corrected area under the speed curve (Fig. 7F, 3rd and 4th panels)—was significantly greater in both Class 1 (Tukey $q = 13.38$, $p < 0.0001$) and Class 3 (Tukey $q = 12.12$, $p < 0.0001$) responses compared to Class 2, regardless of whether it was measured from CS onset or from the avoidance response.

These results indicate that both Class 2 and Class 3 avoids reflect cautious responding, but with distinct behavioral signatures suggestive of different internal states. Class 2 avoids involve ongoing spontaneous movement at CS onset, accompanied by larger orienting responses and a smaller change in speed during avoidance—possibly indicating a distracted but cautious animal already in motion. In contrast, Class 3 avoids are marked by behavioral quiescence at CS onset, minimal orienting, and delayed avoidance, consistent with an alert yet hesitating state in which the animal delays responding until the last moment. Class 1 avoids, by comparison, show rapid onset and large-amplitude orienting responses, typical of animals adapting to dynamic or challenging environments (Zhou et al., 2023).

We next examined how STN activity varied across avoidance classes by averaging the F/F time series from all recorded neurons. This revealed distinct levels of STN activation across the classes (Fig. 7A, top panel, aligned to CS onset; Fig. 7C, aligned to avoidance response). Class 3 avoids exhibited the highest STN activation, measured both from CS onset (Tukey $q = 19.26$, $p < 0.0001$ vs. Class 1; Tukey $q = 16.52$, $p < 0.0001$ vs. Class 2) and from avoidance response (Fig. 7E; Tukey $q = 20.95$, $p < 0.0001$ vs. Class 1; Tukey $q = 15.68$, $p < 0.0001$ vs. Class 2). In contrast, Class 1 avoids showed the lowest STN activation. Importantly, there were no significant differences in STN activity between classes during the CS-evoked orienting response (one-way ANOVA, $F(2,2185) = 0.36$, $p = 0.6943$), indicating that these neurons do not encode orienting per se. Together, these results indicate that STN activation scales with behavioral caution, with the highest activation associated with the most delayed (Class 3) avoidance responses.

We next applied k-means clustering to the F/F time series of individual neurons during each avoidance class, revealing three distinct neuronal activity types per class (Fig. 7B). For

Class 1 avoids, three neuron types were identified: *Type 1a* neurons showed no activation, *Type 1b* neurons exhibited inhibition at CS onset followed by activation during the avoidance response, and *Type 1c* neurons activated during the avoidance response (Tukey $q = 14.88$, $p < 0.0001$, 1c vs. 1a; $q = 8.4$, $p < 0.0001$, 1c vs. 1b). For Class 2 avoids, *Type 2a* neurons showed no activation, *Type 2b* neurons activated during the avoidance response, and Type 2c neurons activated in advance of the response (Tukey $q = 25.39$, $p < 0.0001$, 2b vs. 2a; $q = 37.55$, $p < 0.0001$, 2c vs. 2a; $q = 16.96$, $p < 0.0001$, 2c vs. 2b). Class 3 avoids exhibited similar patterns to Class 2, *Type 3a* neurons showed minimal activation, *Type 3b* neurons activated near the time of movement, and *Type 3c* neurons activated prior to the avoidance response (Tukey $q = 33.49$, $p < 0.0001$, 3b vs. 3a; $q = 41.43$, $p < 0.0001$, 3c vs. 3a; $q = 18.77$, $p < 0.0001$, 3c vs. 3b).

Within each avoidance class, avoidance movements were generally similar regardless of neuron type, with a few exceptions involving *Type a* neurons, which did not activate during avoidance. In Class1, *Type 1a* neurons were associated with higher baseline movement and stronger CS-evoked orienting responses, but lower avoidance movement speeds (from CS onset or from avoidance response) compared to *Type 1b* (Tukey $q=10.55$ $p<0.0001$) and *Type 1c* (Tukey $q=12.25$ $p<0.0001$) neuron types (Fig. 7B,D lower left panel and Fig. 7F, 3rd and 4th panels). In Class 2, *Type 2a* neurons were linked to larger orienting responses than *Type 2b* (Tukey $q = 5.36$, $p = 0.0047$) and *Type 2c* (Tukey $q = 6.67$, $p = 0.0001$) neurons (Fig. 7F, 2nd panel). This indicates that strong orienting responses are associated with reduced STN activation during the ensuing avoidance behavior.

Together, these results reveal two key findings. First, the magnitude of STN activation is closely linked to the class of avoidance response, with stronger activation observed during more cautious behaviors—those with longer latencies to avoid. Second, within cautious trials, distinct

subpopulations of neurons emerge: some (*Type 2b* and *3b*) are active near the time of movement, while others (*Type 2c* and *3c*) activate in advance, potentially contributing to action planning and generation. These patterns suggest that STN activity not only reflects but may also anticipate and facilitate the level of cautious behavior. In particular, stronger and earlier STN activation is associated with slower, more deliberate avoidance responses, consistent with an internal representation of behavioral caution. These findings position the STN as a critical node for orchestrating adaptive, goal-directed actions under threat, particularly in situations that require careful timing of responses.

***STN excitation drives cued actions***

The preceding results indicate that STN neurons activate during signaled active avoidance behavior suggesting an important role in this behavior. Next, we used optogenetics to modulate the activity of STN glutamatergic neurons as mice performed AA1, AA2, and AA3 procedures. To excite STN neurons at varying levels, we expressed ChR2 and applied a spectrum of blue light patterns in STN including trains (1-ms pulses at 2-100 Hz) and continuous (Cont) light. To inhibit STN neurons, we expressed eArch3.0 applying Cont green light at varying power levels. Within each session, we compared randomly delivered CS (control), NoCS (catch), CS+Light, and Light trials. The light was delivered during the avoidance interval and continued during the escape interval if mice failed to avoid in active avoidance trials. In addition, No Opsin mice were subjected to these same trials and compared to opsin expressing mice. Initially, we tested the effects of the optogenetic light (blue and green) in No Opsin mice (n=10) subjected to the behavioral procedures. In the absence of opsin expression, the light (CS vs CS+Light trials) had little effect on behavioral performance (active avoids rate and latency) during AA1

(RMAnova $F(1,9)= 0.16$ $p=0.69$; $F(1,9)= 0.87$ $p=0.37$), AA2 (RMAnova $F(1,9)= 2.65$ $p=0.14$; $F(1,9)= 0.08$ $p=0.78$), or AA3 (2WayRMAnova $F(1,9)= 0.01$ $p=0.9$; $F(1,9)= 0.00005$ $p=0.99$) procedures.

We first tested the effects of exciting glutamatergic STN neurons by expressing ChR2 in the STN of Vglut2-Cre mice with bilateral injections of a Cre-inducible AAV (Fig. 8A; STN-ChR2, n=9 mice). Excitation of STN neurons during AA1 increased the percentage of active avoids (90.2±1.9 vs 97.2±1.5 %; CS vs CS+Light trials) but avoids are close to maximal in control CS trials and the effect only bordered significance (Fig. 8B circles top; Tukey $t(5)= 3.6$ $p=0.051$). However, STN excitation produced by blue light patterns >20 Hz, including Cont, sharply decreased avoid latencies (Fig. 8B circles middle; Tukey $t(5)= 5.19$ $p=0.014$). Movement tracking revealed that the effects of STN excitation (>20 Hz) on AA1 performance were associated with both a strong increase in the orienting response amplitude (Fig. 8C,D left; Tukey $t(10)= 6.47$ $p=0.0027$) and an earlier onset of the ensuing avoid, which peaked sooner measured from CS onset (Fig. 8C,D middle; Tukey $t(10)= 9.94$ $p<0.0001$). However, the peak speed of the avoids measured from the response occurrence was not affected by STN excitation (Fig. 8C,D right; Tukey $t(10)= 0.36$ $p=0.96$). This indicates that STN excitation leads to earlier onset avoids occurring at a similar peak speed as normal avoids. Therefore, instead of the characteristic avoid latencies that occur around the middle of the avoidance interval, avoids occur earlier as a function of STN excitation frequency without altering their peak speed.

To test if STN excitation alone could substitute for the natural CS, we employed Light trials. STN excitation at 10-20 Hz drove active avoids at percentage rates (Fig. 8B triangles top; Tukey $t(10)= 2.55$ $p=0.21$ CS vs Light trials 10-20 Hz) and latencies (Fig. 8B triangles middle; Tukey $t(10)= 0.08$ $p=0.99$) that did not differ from control CS trials indicating that excitation at

these frequencies can generate normal avoidance responses. In contrast, STN excitation >20 Hz drove earlier onset avoid latencies compared to control CS trials (Fig. 8B triangles middle; Tukey $t(10)= 4.76$ $p=0.017$) or lower frequency (<20 Hz) STN excitation Light trials (Tukey $t(10)= 4.84$ $p=0.016$). Movement tracking revealed that STN excitation >20 Hz caused a strong increase in the orienting response (Fig. 8E,F; Tukey $t(10)= 4.7$ $p=0.019$), and an earlier avoid onset (Fig. 8E,F; Tukey $t(10)= 5.42$ $p=0.0085$), but did not change the peak speed of avoids compared to the CS (Fig. 8E,F; Tukey $t(10)= 0.3$ $p=0.976$). Thus, optogenetic STN activation driven by 1-ms blue light pulses at 10-20 Hz drives active avoids at normal speeds and onset latencies that are comparable to the active avoids driven by a natural CS, while stronger STN activation> 20 Hz shifts onset latencies earlier without altering peak speed.

The preceding Light trials occurred in trained mice. Therefore, we tested the effect of STN excitation in a group of naïve STN-ChR2 mice (n=5 mice) to determine if they would innately cross between compartments when STN excitation was applied even though it does not predict the US. During five sessions, we randomly presented NoCS (i.e., catch trials) and NoCS+Light trials (i.e., the light does not predict the US, which is not presented, but crossing stops the light just like an avoid stops the CS). Mice produced a high rate of crossings during STN excitation >20 Hz including Cont (Fig. 9A blue circles; Tukey $t(12)= 5.87$ $p=0.0063$ NoCS vs NoCS+Light >20 Hz). To determine if during the naïve sessions the mice were learning to escape the STN stimulation over days, we compared the rate of crossings during the light between the first session and the fifth session but found no difference (Tukey $t(4)= 0.6$ $p=0.6$ Session 1 vs 5 for NoCS+Light >20 Hz). Thus, mice innately move away when STN is excited at high frequencies >20 Hz, which are the frequencies that drive early onset avoids when presented in CS+Light trials.

On the sixth session, the NoCS+Light trials were converted to Light trials (i.e., the light now predicts the US; 2-5 Hz were excluded to reduce the number of punished trials). This led to an increase in avoidance rates for all STN excitation light patterns (Fig. 9A red triangles; 2WayRMAnova NoCS+Light vs Light trials $F(1,16)=27.7$ $p=0.006$) but this did not affect NoCS trials or ITCs ($F(1,16)=0.58$ $p=0.48$). In particular, Light trials at 10-20 Hz, which did drove few crossings in naïve animals, became as effective as a natural CS at driving active avoids at normal latencies. Light trials >20 Hz were also effective at driving avoids but as for CS+Light trials they were characterized by early onset avoids. Furthermore, the addition of the natural CS to the Light trials (i.e., converting them to CS+Light trials; not shown) had no effect on avoidance rates for Light trials >5 Hz (Tukey $t(32)<2.3$ $p>0.17$ for 10-100 Hz and Cont), indicating that Light alone >5 Hz is equivalent to a natural CS, with 10-20 Hz matching the response features of normal avoids.

These results indicate that optogenetic STN activation at 10-20 Hz serves as a signal as effective as a natural CS in a cued goal-directed task while activation at higher frequencies drives earlier onset avoids without altering their peak speed and 2-5 Hz low frequency STN activation has little effect. STN activation has an intrinsic ability to serve as a CS during signaled active avoidance by associating with the US it predicts.

***STN excitation blocks the development of caution when errors are punished***

During basic signaled active avoidance, which we term AA1, ITCs occur freely without consequence, but the succeeding AA2 procedure punishes ITCs, requiring mice to passively avoid during the intertrial interval. A characteristic, reliable feature of the transition between AA1 and AA2 procedures is a rightward shift of the cued active avoidance action to longer

latencies in an apparent reflection of caution (Zhou et al., 2022). Since STN excitation shifts active avoid latencies earlier or leftward, we tested if STN excitation may interfere with the normal development of longer or rightward latency shifts between AA1 and AA2.

We used STN-ChR2 (n=6) and NoOpsin mice (n=7) subjected only to CS+Light trials (40-66 Hz; Fig. 9B) in successive AA1 sessions followed by AA2 sessions. During AA2, ITCs were rapidly abolished with little effect on active avoid rate but avoidance latencies did not shift longer in STN-ChR2 mice, as they did in control No Opsin mice (Fig. 9B). Thus, the shift in avoid latency was larger in No Opsin mice compared STN-ChR2 mice subjected to STN excitation ($F(1,11)=8.3$ $p=0.01$; STN-ChR2 vs No Opsin). In fact, movement tracking revealed that STN excitation caused a leftward shift of speed during AA2 (Fig. 9C upper), which is earlier and opposite to what occurs in No Opsin (Fig. 9C lower) or normal mice (Zhou et al., 2022). These results indicate that STN excitation >20 Hz is incompatible with the normal development of cautious behavior about generating a CS signaled action (action) when the occurrence of the unsignaled action (ITC) is punished.

***STN excitation is incompatible with passive avoidance***

In the preceding experiments, we tested the effects of STN excitation on CS signaled active avoids by applying optogenetic light during the active avoidance interval. To test the effect of STN excitation on passive avoidance, we used the AA3 procedure. During AA3, mice discriminate between two different tones (CS1 and CS2) delivered randomly; CS1 signals an active avoidance interval (like the CS in AA1/2), while CS2 signals a passive avoidance interval when mice are punished for crossing to the other compartment (ITCs are not punished). During

AA3, mice must produce opposite actions to CS1 (active) and CS2 (passive). Thus, crossings (active avoids) during CS2 are errors.

In STN-ChR2 mice (n=11), we compared errors in control CS2 trials versus CS2+Light trials when STN excitation (40-66 Hz) is delivered during the passive avoidance interval. In later sessions, we also tested NoCS+Light trials, when the STN excitation occurs alone without consequence. Mice discriminated between CS1 and CS2 trials by performing high rates of active avoids to CS1 and virtually nil to CS2, indicating their ability to passively avoid during CS2 (Fig. 9D; Tukey $t(30)= 13.65$ $p<0.0001$ CS1 vs CS2). However, STN excitation in CS2+Light trials blocked passive avoids causing mice to err (cross) on most of these trials (Fig. 9D; Tukey $t(30)= 13.63$ $p<0.0001$ CS2 vs CS2+Light). This occurred despite being punished for these errors. In fact, there was no difference in the rate of active avoids between CS2+Light trials and CS1 trials (85.2±2 vs 85.2±8; Tukey $t(30)= 0.01$ $p=0.99$ CS1 vs CS2+Light). Moreover, STN excitation alone in NoCS+Light trials drove the same high rate of active avoids as CS1 and CS2+Light trials (Fig. 9D; Tukey $t(30)= 0.21$ $p=0.99$ NoCS+Light vs CS2+Light), even though this did not predict the US and was not punished.

Movement tracking showed that the orienting response evoked by CS2, which can be small or even inhibitory (Zhou et al., 2023), was enhanced by STN excitation (Fig. 9E,F; Tukey $t(30)= 11.62$ $p<0.0001$ CS2 vs CS2+Light). The movement evoked by CS2 was also enhanced by STN excitation in association with the errors (Fig. 9E,F; Tukey $t(30)= 11.79$ $p<0.0001$ CS2 vs CS2+Light). In addition, because the mice are punished for crossing during CS2+Light trials, there was more movement during these trials related to the delivery of the punishment compared to NoCS+Light trials (Tukey $t(30)= 3.92$ $p=0.04$), which are not punished. This is noticeable by a hump in the speed trace of CS2+Light trials after the response error (red trace in Fig. 9E From

response). Interestingly, when punished for these errors, mice move rapidly in reaction to the US but do not cross back to the other compartment, as indicated by the fact that the number of ITCs is virtually nil. These results indicate that STN excitation is incompatible with passive avoidance, and STN may serve as an important hub to regulate this inhibitory action.

In conclusion, optogenetic STN activation >20 Hz drives signaled active avoids earlier, shifting the cued action latency earlier and is incompatible with both cued inhibitory actions, such as passive avoidance, and the normal expression of caution when the occurrence of the action uncued is punished. These fast onset actions are typical of approach responses motivated by rewards or escape responses driven by the presence of an aversive stimulus. It is difficult to identify the nature of the sensation and the type of action (approach vs escape) caused by this high level of STN activation in mice, and this was not pursued further in the current study. Importantly, STN activation at 10-20 Hz drives normal signaled active avoidance responses indicating that STN may be involved in generating normal cued actions and this can only be addressed by testing the impact of reducing STN activation.

**STN excitation is not aversive**

Given that STN excitation produces fast responses, it has been proposed that such stimulation might be aversive (Serra et al., 2023). Signaled active avoidance, in which a sensory cue predicts an aversive event, provides an ideal paradigm to test whether STN excitation is itself aversive and can function as a US. To address this, we trained naïve mice expressing ChR2 in STN neurons (with bilateral STN cannulas) using a modified AA1-3 procedure, where three CSs (CS1–CS3) were introduced from the first AA1 session. In this version, the US was STN excitation delivered as 66 Hz blue light (1-ms pulses) at ~1.5 mW, titrated for each animal (n =

9) to reliably evoke rapid (<1.5 s) escape responses, comparable to those elicited by the standard aversive US. Control mice lacking opsin expression (No Opsin) were trained under the same conditions, including light delivery (n = 7).

During AA1, CS1 predicts the US light, while CS2 and CS3 predict nil. Crossing during CS1-3 turns off the CS and in CS1 avoids the light US. During AA2, intertrial crossings were punished by the light US (0.5 sec). During AA3, crossing during presentation of CS2 resulted in light US punishment (0.5 sec). Despite the robust light-evoked escape responses during the US interval, ChR2-expressing mice failed to learn active avoidance to CS1 in AA1, AA2, or AA3 procedures (Fig. 10A). There was no difference in any of the measured parameters between the Opsin and the No Opsin groups (Mixed ANOVA Interaction GroupxCS; Tukey's p>0.8 Opsin vs No Opsin during AA1-3). The CS1 cue, which predicted the STN excitation, did not increase avoidance behavior compared to CS2 or CS3, which were not predictive. In AA2, where intertrial crossings were also punished with STN excitation (0.5 sec), there was no reduction in these crossings. Similarly, during AA3, STN excitation failed to suppress crossings during CS2, which were also punished by the light. Mice had large numbers of crossings or spurious active avoids (~45%) that were similar among the three CS's despite the differences in the contingencies they predict, which is also indicative of normal exploratory behavior in an environment that is not punitive.

However, when the same mice were trained in the standard AA1 procedures using the regular aversive US (footshock and white noise), they rapidly learned to avoid during CS1 and significantly reduced crossings during CS2 and CS3—especially during AA2 and AA3, where these responses were punished (Fig. 10B). There was a small difference in the percentage of avoidance responses in Opsin vs No Opsin mice during AA2 and AA3 but not AA1 (Mixed

ANOVA Interaction GroupxCS; Tukey q(28)=5.7 p=0.004 Opsin vs No Opsin during AA2; Tukey q(28)=4.3 p=0.044 during AA3) indicating that the mice had learned something about the CS1 predicting the STN excitation during the light US sessions, which reduced their avoids during the more cautious versions of the regular aversive tasks, perhaps emphasizing the role of STN in the more cautious responding that emerges during these sessions. In conclusion, these findings indicate that STN excitation, as applied in this study, does not function as an aversive US. Rather, the fast escape responses it elicits appear to result from its role in movement initiation, not from negative valence.

***STN inhibition blocks signaled active avoidance***

The preceding STN excitation experiments suggest that STN activation may have an important role in mediating signaled active avoidance. If this is the case, signaled avoidance should be impaired by optogenetically inhibiting STN. To inhibit glutamatergic STN neurons, we expressed eArch3.0 in the STN of Vglut2-Cre mice with bilateral injections of a Cre-inducible AAV (STN-Arch, n=6 mice).

We found that inhibiting STN neurons in CS+Light trials suppressed the percentage of active avoids compared to CS trials as a function of green light power during AA1, AA2 and AA3-CS1 (Fig. 11A). Active avoids were suppressed by all powers tested; at the higher light powers (≥15 mW), avoids were strongly suppressed (Tukey t(5)= 11.65 p=0.0004 CS vs CS+Light). When avoids failed, STN inhibition did not suppress the occurrence of escape responses evoked by the US; the mice escaped rapidly at US onset on every failed avoid trial (7 sec from CS onset). Thus, STN inhibition selectively suppressed avoidance responses, not escape responses. In AA1, some mice increased the number of ITCs during the intertrial interval

following a failed avoid caused by STN inhibition (Fig. 11A bottom panel, Tukey $t(5)= 10.28$ $p=0.0008$), which is a common coping strategy when ITCs are not punished. We also tested if STN inhibition impairs passive avoids in AA3 and found that the number of errors in CS2+Light trials was not different than in control CS2 trials (Fig. 11A; Tukey $t(9)=0.83$ $p=0.9$).

Measurements of peak speed (baseline corrected) during AA1, AA2 and AA3-CS1 showed that STN inhibition slightly increased the orienting response (Fig. 11B,C; Tukey $t(5)= 5.76$ $p=0.0096$) but this was followed by a suppression of action speed (Fig. 11B,C; Tukey $t(5)= 5.06$ $p=0.016$) in association with the abolishment of avoids. However, mice escaped rapidly upon US onset. Neither the peak speed (Tukey $t(5)= 0.6$ $p=0.6$) nor the time-to-peak speed (Tukey $t(5)= 0.9$ $p=0.5$) of escapes was affected by STN inhibition, indicating that STN inhibition did not paralyze the mice or impair their ability to cross. The movement during the passive avoidance interval in AA3-CS2 trials was somewhat inhibited by STN inhibition (Tukey $t(4)=4.67$ $p=0.04$), which would facilitate passive avoidance.

These results indicate that STN glutamatergic neuron activation is essential for signaled active avoidance.

***STN lesions impair active avoidance but not passive avoidance actions***

The optogenetic experiments indicate that STN is essential for cued active avoidance actions. We decided to use lesions of STN to verify these results and to test additional issues. First, we determined if the lesion impaired active and passive avoidance learning. Second, we determined if the lesion impaired performance of unsignaled passive avoidance (when ITCs are punished in AA2).

To determine if STN neurons are important for learning avoidance behaviors, we bilaterally injected AAV8-EF1a-mCherry-flex-dtA into the STN of Vglut2-cre mice (n=12) to lesion STN glutamatergic neurons. To verify the lesion, we counted the number of neurons (Neurotrace) in the STN of lesion and control mice and found that the AAV injection reduced the number of STN neurons (Fig. 12A, Mann-Whitney Z=6.45 p<0.0001 Lesion vs Control). The lesion had a strong negative effect on signaled active avoidance tasks (Fig. 12B) compared to control mice (n=6) and to a group of zona incerta lesion mice from a previous study (Hormigo et al., 2023) that underwent the same procedures as the STN lesion mice but the AAV was injected in Vgat-Cre mice thereby lesioning GABAergic neurons in the adjacent zona incerta without causing significant impairment in the same tasks. Combining the AA1, AA2 and AA3-CS1 sessions together, we found that the percentage of active avoids was impaired in STN lesion mice compared to both control (ANOVA Tukey t(18)= 5.68 p=0.002) and zona incerta lesion mice (Tukey t(18)= 5.04 p=0.005). In contrast, the number of ITCs did not differ between the groups (ANOVA F(2,18)=1.04 p=0.37), and there was no difference in the percentage of errors in AA3-CS2 between the three groups (ANOVA F(2,18)= 0.23 p=0.79). Thus, signaled active avoidance was selectively impaired, as spontaneous crossings and passive avoidance were spared.

We also compared movement during task performance for the three procedures (AA1, AA2 and AA3-CS1) and found that in STN lesion mice compared to control mice there was an increase in the peak amplitude of the orienting response (ANOVA  Tukey t(10)=4.2 p=0.01) and a decrease in avoidance interval movement measured either from CS onset (Tukey t(10)=8.3 p=0.0001) or from response occurrence (Tukey t(10)=8.3 p=0.0001). Finaly, the movement during passive avoids in AA3-CS2 trials did not differ between control and lesion mice (Fig.

11D; Tukey $t(10)= 1.5$ $p=0.28$). In conclusion, selective lesions of STN glutamatergic lesions impaired signaled active avoidance learning and performance.

Since the AAV-based lesion may leave some STN cells intact, we performed electrolytic lesions of STN (Fig. 12F), which assures elimination of STN cells. We tested the effect of the lesion in trained mice (n=13; Fig. 12G) using a repeated measures design, and the lesion mice were also compared to control mice (n=6). The lesion impaired the percentage of active avoids in AA1 (Tukey $t(36)= 5.18$ $p=0.0043$ before vs after the lesion) and especially in AA2 (Tukey $t(36)= 11.7$ $p<0.0001$) when ITCs are punished. Mice continued to perform ITCs after the lesion in AA1 albeit at a lower rate (Tukey $t(36)= 6.47$ $p=0.0003$ AA1 before vs after lesion), and ITCs were further suppressed during AA2 (Tukey $t(36)= 7.4$ $p<0.0001$ AA1 vs AA2 after lesion). During AA3, which requires discriminating between CS1 and CS2 to select the appropriate action, mice continued to be impaired in active avoidance (AA3-CS1) but the percentage of errors during CS2 in lesion mice was not higher than in control mice (Mixed Anova Tukey $t(36)=0.23$ $p=0.99$ Control vs Lesion for AA3-CS2).

These results indicate that STN lesions impair signaled active avoidance performance, but do not increase signaled passive avoidance errors. In the context of typical Go/NoGo tasks, STN integrity is important for the Go portion the task (AA1-3), while the NoGo portion requiring action inhibition or postponement (unsignaled and signaled passive avoidance in AA2/3), and the discrimination (AA3) between the two stimuli signaling the different contigencies do not seem to be dependent on STN.

***STN projections to the midbrain are required for cued active avoidance***

The results indicate that glutamatergic STN neurons have a critical role in signaled active avoidance. STN neurons have both ascending projections to the GPe area, and descending projections to SNr and the tegmentum in the midbrain (Kita and Kitai, 1987; Friedman and Yin, 2023; Prasad and Wallen-Mackenzie, 2024). Thus, we compared the effect of exciting the fibers of STN neurons ascending to GPe and descending in midbrain.

We prepared Vglut-STN-ChR2 mice but implanted the optical fibers in the GPe area (GPe group, n=7 mice), or in the SNr/tegmentum areas (Midbrain group, n=8 mice). The two sites in the midbrain were combined because the effects of exciting these areas were similar. A third combined No Opsin group (n=5 mice) had optical fibers implanted in the same targets as the other two groups. The locations of the optical fiber endings for these groups are depicted in Figure 13A.

We first explored if excitation of the STN pathways to GPe or midbrain drove earlier onset active avoid latencies characteristic of STN excitation. In CS+Light trials during AA1 (Fig. 13B; MixedAnova Group x Light), we found that excitation of STN fibers in the midbrain produced earlier onset latency active avoids than excitation of STN fibers in GPe (Tukey $t(41)=5.2$ $p=0.001$) or compared to the NoOpsin (Tukey $t(41)=4.4$ $p=0.008$) mice. The light patterns that were effective in driving earlier onset avoids were only the high frequency trains (40-100 Hz), which is consistent with these patterns being the most effective at activating fibers in a sustained fashion (Hormigo et al., 2019; Hormigo et al., 2021a; Hormigo et al., 2021c).

Next, we tested the development of caution reflected by the signaled action timing during the transition between AA1 and AA2 when all trials are CS+Light trials (40-66 Hz or Cont; Fig. 13C). We found that excitation of STN projections to the midbrain, but not those to GPe or in No

Opsin mice, blocked the development of caution (Fig. 13C; MixedAnova Group x AA1/2). In all the groups, the ITCs were abolished during AA2. As occurs in control mice, in the No opsin (Tukey $t(6)= 7.1$ $p=0.0024$) and GPe (Tukey $t(5)= 6.31$ $p=0.0066$ AA1 vs AA2) groups the active avoid latencies shifted longer between AA1 and AA2. However, this shift did not occur in the midbrain group (Tukey $t(7)= 1.5$ $p=0.3252$) indicating that activation of the STN pathways to midbrain interferes with the development of caution when the unsignaled action is punished.

We then tested the effects of STN fiber excitation on signaled passive avoidance during AA3. Only excitation of STN pathways to the midbrain, but not those to GPe or the NoOpsin mice, blocked passive avoids to CS2 (Fig. 13D) by increasing the rate of errors to CS2 (Tukey $t(63)= 7.81$ $p=0.0001$ CS2 vs CS2+Light) to levels that were equivalent to CS1 (Tukey $t(63)= 2$ $p=0.98$ CS1 vs CS2+Light) despite the fact that these CS2 errors are punished. Moreover, the increase in crossings caused by activating STN pathways to midbrain also occurred in NoCS+Light trials, which were not different compared to CS2+Light trials (Tukey $t(63)= 0.78$ $p=1$ CS2+Light vs NoCS+Light).

Finally, we explored if these pathways could serve as an effective CS to drive active avoids in the absence of a natural auditory stimulus. In Light trials during AA1, we found that excitation of STN projections to the midbrain, but not those to GPe, were able to drive high rates of active avoids equivalent to the natural CS (Fig. 13E; MixedAnova Group x Light). Thus, activation of STN projections to the midbrain (Tukey $t(38)>7$ $p=0.0007$) at either 20-100 Hz or Cont drove higher rates of active avoids compared to GPe. Moreover, there were no differences in active avoid rates between the GPe and midbrain projection groups when they were activated at the lower 2-10 Hz optogenetic frequencies or when a natural CS was used.

Taken together, these results indicate that activation of STN pathways descending to the midbrain are responsible for the effects we observed when glutamatergic STN neurons were excited. To test if the activation of this pathway is necessary for signaled active avoidance, we expressed eArch3.0 in STN-Arch mice (n=11) but placed the optical fibers in the midbrain to inhibit STN fibers coursing to the midbrain. A group of No Opsin mice (n=5) also had optical fibers in the midbrain. Inhibiting STN fibers in the midbrain with green light during AA1, AA2 and AA3-CS1 CS+Light trials suppressed the percentage of active avoids compared to CS trials in STN-Arch but not in No Opsin mice (Fig. 14A; Mixed Anova Light x Group; Tukey $t(14)=7.03$ $p=0.0008$ STN-Arch vs No Opsin for CS+Light trials). Inhibition of STN fibers in the midbrain did not affect escape responses; the mice escaped rapidly at US onset on every failed avoid trial. Furthermore, STN fiber inhibition in the midbrain did not affect the percentage of passive avoids in AA3-CS2 trials (Fig. 14A right panel; Tukey $t(30)=2.5$ $p=0.64$ CS vs CS+Light in STN-Arch mice).

Measurements of peak speed (baseline corrected) during AA1, AA2 and AA3-CS1 showed that STN inhibition did not affect the orienting response (Fig. 14B,C) but there was a suppression of action speed (Fig. 14B,C; Tukey $t(14)= 5.08$ $p=0.01$ CS+Light vs CS trials in STN-Arch mice) in association with the abolishment of avoids. However, mice escaped rapidly upon US onset. The peak speed of escapes was not affected by STN fiber inhibition (Tukey $t(13)= 0.22$ $p=0.99$ CS+ Light vs CS trials in STN-Arch mice), indicating that STN inhibition did not paralyze the mice or impair their ability to cross. The movement during the passive avoidance interval in AA3-CS2 trials was somewhat inhibited by STN inhibition (Tukey $t(10)=4.48$ $p=0.04$), which would facilitate passive avoidance. These results indicate that STN glutamatergic neuron pathways to the midbrain are essential for signaled active avoidance.

## Discussion

This study investigated the role of STN in goal-directed behavior and movement dynamics, focusing on the function of STN glutamatergic neurons through a combination of neural activity recording and manipulation techniques. Our findings reveal that STN circuits encode movement direction and goal-directed active avoidance actions. In addition, STN activity is essential for generating cued active avoidance actions. We show that STN neurons activate during active avoidance movements and exhibit their strongest activation in anticipation of cautious responses—those characterized by delayed onsets but rapid executions. Manipulating STN activity controls the timing of avoidance responses disrupting cautious responding by advancing action onset in a frequency-dependent manner without affecting peak speed. Heightened STN activation also interferes with passive actions, rendering it incompatible with passive avoidance. Importantly, these effects are not due to aversion but appear to result from movement induction. Conversely, both irreversible STN lesions and reversible inactivation of the STN or its projections to the midbrain—but not to the GPe—effectively block signaled active avoidance, highlighting the critical role of these circuits in the performance of learned avoidance behaviors. Our findings establish that STN activates during cued actions and is essential to generate these movements.

### *Directional Movement Bias*

We found that STN neurons discharge during self-paced movement onset and active but not passive avoidance actions, which is consistent with recent results showing that STN neurons increase firing during self-paced locomotion in head-fixed mice (Callahan et al., 2024). In

addition, we found evidence of directional movement bias linked to STN activation by exciting and recording these neurons. First, unilateral STN excitation in an open field induced ipsiversive movements, with the directional bias scaling as a function of the excitation. Interestingly, studies that disagree on the effects of bilateral STN excitation on movement, as either enhancing (Friedman and Yin, 2023) or inhibiting movement (Guillaumin et al., 2021), agree that unilateral STN excitation causes ipsiversive movements. Second, our recordings showed that STN activation is preferentially associated with contraversive movements suggesting a direction-specific role for the STN in motor output. However, the fact that excitation of STN neurons produces an ipsiversive movement bias complicates this interpretation. If STN activation were a pure motor signal for contraversive movements, excitation should drive contraversive actions. This apparent contradiction—STN activity encoding contraversive movements but driving ipsiversive movements—suggests that STN activation may not represent a direct motor-driving signal. Instead, it may encode a "move-away" signal, reflecting the need to vacate the contralateral space (represented by STN activity due to lateralization). This interpretation could be consistent with the idea that STN excitation may have aversive qualities (Serra et al., 2023) but a move away signal does not need to be aversive. It may simply represent the activation of a network that drives these movements. The ipsiversive bias produced by STN excitation is consistent with the effects of directly exciting one of its main targets, GABAergic neurons in the SNr, which also produce ipsiversive movements in the same arena under the same conditions (Hormigo et al., 2021a). This implies that the ipsiversive movements caused by STN excitation are a simple consequence of exciting SNr and other targets that cause movements in the ipsiversive direction. However, as discussed below, while the effects of unilaterally exciting

STN and SNr on movement bias are congruent, the effects of bilaterally exciting these nuclei on cued actions are not congruent.

In conclusion, the lateralized contraversive encoding revealed during spontaneous orienting movements may reflect the initiation of movements away from contralateral space. In this scenario, bilateral STN activation would drive linear, translational actions away from the current location, which depending on the situation can be towards a rewarding location in appetitive contexts or away from a location in avoidance contexts. Thus, the STN circuit may function as a central forebrain mechanism for generating goal-directed actions, such as active avoidance or approach, which at higher levels of activation are incompatible with passive or inhibitory actions, such as passive avoidance or staying put.

### *Effects of STN Excitation on Cued Actions*

Evidence in humans shows that low-frequency oscillatory activity from the prefrontal cortex communicates with the STN to increase decision thresholds, promoting more deliberative—and thus slower, less impulsive—actions (Frank et al., 2007). In contrast, high-frequency STN DBS in Parkinson's patients disrupts these signals, lowers decision thresholds, and induces impulsive decisions (Cavanagh et al., 2011; Herz et al., 2018; Herz et al., 2024; Pagnier et al., 2024). In close agreement with these findings, we show that optogenetic stimulation of the STN in mice decreases goal-directed response latencies in a frequency-dependent manner.

When examining the effects of STN excitation on behavior, our study includes two key features. First, we tested a wide range of optogenetic excitation patterns to modulate STN activity, uncovering differential effects that prior studies, often limited to a single stimulation

pattern, may have missed. Second, we used a cued active avoidance task, where mice characteristically respond with slow onsets. This design enabled us to capture the impact of STN excitation at varying frequencies on action timing. These effects could be overlooked in appetitive tasks due to the rapid onset of approach actions (Zhou et al., 2022).

Optogenetic STN excitation at medium frequencies (10–20 Hz) generated active avoidance responses closely resembling those triggered by a natural CS, matching in both timing and peak speed. In contrast, high-frequency excitation (>20 Hz) advanced action onset but did not increase peak speeds. Moreover, high-frequency stimulation evoked spontaneous crossings in untrained mice, suggesting an innate escape-like response to intense STN activation. In contrast, lower-frequency excitation did not induce spontaneous responses but effectively generated normal avoidance behaviors when STN activation served as a predictive CS for the US.

These findings align with STN's purported role in action initiation in mice (Watson et al., 2021; Callahan et al., 2024), but the effects of high-frequency excitation may reflect the aversive nature of excessive STN activation (Serra et al., 2023). Deciphering the exact sensation elicited by STN excitation in mice is challenging, particularly since even self-stimulation rewarding brain sites can become aversive under intense stimulation (Valenstein and Valenstein, 1964). A key distinction between escape behaviors driven by aversive stimuli and avoidance actions is the increased peak speed characteristic of escapes (Zhou et al., 2022; Hormigo et al., 2023; Zhou et al., 2023). However, high-frequency excitation primarily shifted response onset earlier without increasing peak speed. This lack of increased peak speed suggests that the effects of STN excitation are not purely aversive.

To directly test whether STN excitation is aversive, we used high-frequency STN stimulation that induces fast escape responses –akin to an aversive US—as the US in signaled

active avoidance procedures. If STN activation were aversive, it should substitute for the natural US and support conditioned avoidance. However, auditory cues that predicted STN excitation failed to drive avoidance responses, indicating that STN activation is not aversive. Notably, those same cues rapidly acquired the ability to drive avoidance when they were subsequently paired with a naturally aversive US.

Our results indicate that STN activation supports normal cued actions at lower levels of excitation, while higher excitation accelerates action onset in a manner that could be misinterpreted as aversive. These findings support a model in which STN activity promotes action initiation and fine-tunes the timing of goal-directed behaviors across contexts—from rapid-onset escape or approach responses to more deliberate, slower-onset avoidance actions where risk evaluation, outcome prediction, and inhibition of premature responses are critical.

***STN is essential for cued avoidance actions***

A key finding of our study is that optogenetic inhibition of STN neurons impairs signaled active avoidance actions without significantly affecting the ability of mice to escape the US, despite both behaviors requiring the same shuttling movement. This effect was corroborated by results from both AAV-mediated and electrolytic STN lesions. Furthermore, inhibition of STN projections to the midbrain tegmentum—but not to the GPe—also impaired active avoidance. These findings demonstrate that STN activation is critical for generating cued goal-directed actions, supporting the idea that the STN functions as an action center working in coordination with the midbrain tegmentum, which is likewise essential for mediating these goal-directed behaviors (Hormigo et al., 2019).

The finding that STN is essential for cued active avoidance actions is underscored by the observation that similar methods to inhibit or lesion related brain areas, such as zona incerta (Hormigo et al., 2020; Hormigo et al., 2023), nucleus accumbens (Zhou et al., 2024), or STN's target in SNr (Hormigo et al., 2016; Hormigo et al., 2021a; Hormigo et al., 2021c), does not impair these behaviors. While these regions can modulate avoidance responses via their direct GABAergic inhibitory projections to the midbrain tegmentum, they are not essential for mediating these actions. Moreover, since SNr inhibition does not suppress signaled avoidance (Hormigo et al., 2021c), it is unlikely that the STN generates avoidance responses by robustly exciting the SNr, as this strongly suppresses active avoidance. Instead, our findings support a model in which the STN drives actions through its direct projections to the midbrain tegmentum. This does not preclude the STN from generating other movements, such as self-paced actions, through its connections with the SNr (Klaus et al., 2019). However, the execution of cued avoidance actions—characterized by slow onset timing—appears to specifically depend on STN's direct pathways to the midbrain tegmentum.

We propose that STN neuron projections to the midbrain tegmentum are essential for mediating cued avoidance actions, functioning independently of its projections to GPe. While the activation imposed by the STN on the SNr during cued actions may serve a modulatory but non-essential role, its direct projections to the midbrain tegmentum may be the critical pathway for generating these actions.

***Influence of STN during inhibitory actions***

Our findings show that high-frequency STN activation disrupts cued passive avoidance in the AA3 discrimination task, where CS1 signals Go (active avoidance) and CS2 signals NoGo

(passive avoidance), resembling typical Go/NoGo procedures used in humans. When STN activation was applied during CS2, mice failed to inhibit their actions and responded to CS2 as though it were CS1. This suggests a direct mechanism by which STN activation can drive inappropriate responding in cued contexts, even when such responses lead to negative outcomes. Notably, similar disruptions of STN function may underlie pathological conditions in which inappropriate actions override goal-directed inhibition, as observed in mouse models of OCD (Parolari et al., 2021; Malgady et al., 2023). This may help explain the therapeutic efficacy of STN DBS in alleviating OCD symptoms in humans (Mallet et al., 2008).

Viral and electrolytic lesions resulted in deficits in cued active avoidance. However, the ability to withhold responses during the intertrial interval, when uncued actions are punished in AA2, remained mostly unaltered. Likewise, these lesions did not increase error rates during CS2 in AA3. This preservation of passive actions might reflect a default NoGo state when STN is inhibited, consistent with its role in cued active avoidance actions. It is noteworthy that we did not investigate conditions where previously triggered actions must be cancelled (Aron, 2011), partly due to our finding that inhibiting STN suppresses the initiation of cued actions. Cued avoidance actions can be set up to test this directly in future work.

An interesting aspect of our study is the impact of STN excitation on cautious behavior, specifically response timing when ITCs are punished (Zhou et al., 2022). The level of STN activation determined the timing of cued actions, with excessive excitation proving incompatible with the normal adjustment of response timing under punishment conditions. This suggests that heightened STN activity impairs behavioral flexibility and the ability to adapt in tasks requiring response inhibition. These findings also align with the proposed role of STN in action slowing and cautiousness under conditions of conflict or difficulty in humans (Frank et al., 2007;

Cavanagh et al., 2014; Herz et al., 2024). Our results indicate that when STN activity is fixed or elevated to high levels, subjects lose the ability to modulate action timing in response to behavioral demands. This has important implications for understanding action control in both typical and pathological states, underscoring the potential of STN as a critical target for regulating action timing in mental health disorders.

Overall, these results strongly support the role of the STN in initiating and regulating the timing of movements in response to learned cues. The preserved passive avoidance suggests that, while the STN is crucial for initiating actions in response to potential threats, it may not be essential for behaviors that rely on default response withholding.

***Implications for STN Function in Adaptive Behavior: Encoding vs Excitation Dissociation***

Our findings demonstrate that STN circuits are essential for cued active avoidance actions, establishing the STN as a central forebrain hub in adaptive avoidance circuitry that integrates inputs from diverse sources to specify these actions. The differential engagement of STN neurons in movement encoding versus movement generation suggests that the STN's role extends beyond issuing a simple motor command. Rather, STN activity may encode a "move away" signal from the lateralized body space it represents, playing a critical role in generating avoidance actions in threat contexts.

This dissociation between encoding and excitation was particularly evident during cued goal-directed actions. Intriguingly, the strongest activation of STN neurons was observed during the most delayed, cautious responses—not during rapid-onset actions. Thus, while STN excitation can drive earlier onset actions as a function of stimulation frequency, our recordings reveal that the STN exhibits maximal excitation during the slowest responses. This finding may

indicate that the highest frequency stimulation, which induces fast responses, reflects a pathological condition of dysregulated STN activity. Indeed, the conflict between STN excitation and passive avoidance underscores the importance of balanced STN function for behavioral adaptability. Excessive excitation appears to disrupt the cautious responses or passive actions that are essential in certain contexts—a dysregulation that may contribute to the impaired behavioral control observed in various mental health disorders.

In conclusion, our study supports a model in which the STN plays a pivotal role in cued avoidance behavior by initiating timed actions in response to threat-related cues through its projections to the midbrain. Unlike other basal ganglia nuclei that may encode these actions, the STN is essential for generating cued responses in collaboration with circuits in the midbrain tegmentum. These findings deepen our understanding of how brain circuits generate adaptive motor responses to avoid harm, a fundamental behavior conserved across species, including humans.

## Materials and Methods

### *Experimental Design and Statistical Analysis*

The methods used in the present paper were like those employed in our previous studies (e.g., (Hormigo et al., 2023; Zhou et al., 2024)). All procedures were reviewed and approved by the institutional animal care and use committee and conducted in adult (>8 weeks) male and female mice. Most experiments involved a repeated measures design in which the mice or cells serve as their own controls (comparisons within groups), but we also compared experimental groups of mice or cells between groups (comparisons between groups). For comparisons within groups, we tested for a main effect of a variable (e.g., Stimulus) using a repeated measures ANOVA or a linear mixed-effects model with fixed-effects and random-effects (e.g., sessions nested within the Subjects as per Data ~Stimulus + (1|Subjects/Sessions lme4 syntax in R) followed by comparisons with Tukey's test. For comparisons between different groups, we used the same approach but included the Group as an additional fixed-effect (Data ~Group*Stimulus + (1|Subjects/Sessions)). Using the standard errors derived from the model, Tukey tests were conducted for the effect of the fixed-effect factors (within group comparisons) or for the Group-Stimulus interaction (between group comparisons). We report the Tukey values for the relevant multiple comparisons.

To enable rigorous approaches, we maintain a centralized metadata system that logs all details about the experiments and is engaged for data analyses (Castro-Alamancos, 2022). Moreover, during daily behavioral sessions, computers run experiments automatically using preset parameters logged for reference during analysis. Analyses are performed using scripts that automate all aspects of data analysis from access to logged metadata and data files to population statistics and graph generation.

***Strains and Adeno-Associated Viruses (AAVs)***

To record from glutamatergic STN neurons using calcium imaging, we injected a Cre-dependent AAV (AAV5-syn-FLEX-jGCaMP7f-WPRE (Addgene: $7x10^{12}$ vg/ml) in the STN of Vglut2-cre mice (Jax 028863; B6J.129S6(FVB)-Slc17a6$^{tm2(cre)Lowl}$/MwarJ) to express GCaMP6f/7f. An optical fiber or GRIN lens was then placed in this location. To inhibit glutamatergic STN neurons using optogenetics, we expressed eArch3.0 by injecting AAV5-EF1a-DIO-eArch3.0-EYFP (UNC Vector Core, titers: $3.4x10^{12}$ vg/ml) in the STN of Vglut2-cre mice (STN-Arch mice). To excite glutamatergic STN neurons using optogenetics, we injected AAV5-EF1a-DIO-hChR2(H134R)-eYFP (UPenn Vector Core or Addgene, titers: $1.8x10^{13}$ GC/ml by quantitative PCR) in the STN of Vglut2-cre mice (STN-ChR2 mice). To kill glutamatergic STN neurons, we injected AAV8-EF1a-mCherry-flex-dtA (Neurophotonics: $1.3x10^{13}$ GC/ml) into the STN of Vglut2-cre mice. No-Opsin controls were injected with AAV8-hSyn-EGFP (Addgene, titers: $4.3x10^{12}$ GC/ml by quantitative PCR) or nil in the STN. For optogenetics, we implanted dual optical fibers bilaterally in the STN or its projection targets. All the optogenetic methods used in the present study have been validated in previous studies using slice and/or in vivo electrophysiology (Hormigo et al., 2016; Hormigo et al., 2019; Hormigo et al., 2021a; Hormigo et al., 2021c).

***Surgeries***

Optogenetics and fiber photometry experiments involved injecting 0.2-0.4 µl AAVs per site during isoflurane anesthesia (~1%). Animals received carprofen after surgery. The stereotaxic coordinates for injection in STN are (from bregma; lateral from the midline; ventral

from the bregma-lambda plane in mm): 2.1 posterior; 1.7; 4.2. In these experiments, a single (400 µm in diameter for fiber photometry or 600 µm lens for miniscope) or dual (200 µm in diameter for optogenetics) optical fiber was implanted unilaterally or bilaterally during isoflurane anesthesia. The stereotaxic coordinates for the implanted optical fibers (in mm) are: STN (2-2.1 posterior; 1.5; 4.2-4.3), midbrain (3.3-3.7 posterior; 1.5; 2.9-4.1), and GPe (0.5 posterior; 2; 3.2). The coordinate ranges reflect different animals that were combined because the coordinate differences produced similar effects. No Opsin mice were implanted with cannulas in STN or its projections sites and the results were combined after confirming that light produced similar effects in these animals.

***Active Avoidance tasks***

Mice were trained in a signaled active avoidance task, as previously described (Hormigo et al., 2016; Hormigo et al., 2019). During an active avoidance session, mice are placed in a standard shuttle box (16.1" x 6.5") that has two compartments separated by a partition with side walls forming a doorway that the animal must traverse to shuttle between compartments. A speaker is placed on one side, but the sound fills the whole box and there is no difference in behavioral performance (signal detection and response) between sides. A trial consists of a 7 sec avoidance interval followed by a 10 sec escape interval. During the avoidance interval, an auditory CS (8 kHz 85 dB) is presented for the duration of the interval or until the animal produces a conditioned response (avoidance response) by moving to the adjacent compartment, whichever occurs first. If the animal avoids, by moving to the next compartment, the CS ends, the escape interval is not presented, and the trial terminates. However, if the animal does not avoid, the escape interval ensues by presenting white noise and a mild scrambled electric foot-

shock (0.3 mA) delivered through the grid floor of the occupied half of the shuttle box. This unconditioned stimulus (US) readily drives the animal to move to the adjacent compartment (escape response), at which point the US terminates, and the escape interval and the trial ends. Thus, an *avoidance response* will eliminate the imminent presentation of a harmful stimulus. An *escape response* is driven by presentation of the harmful stimulus to eliminate the harm it causes. Successful avoidance warrants the absence of harm. Each trial is followed by an intertrial interval (duration is randomly distributed; 25-45 sec range), during which the animal awaits the next trial. We employed four variations of the basic signaled active avoidance procedure termed AA1, AA2, AA3 and AA4.

In AA1, mice are free to cross between compartments during the intertrial interval; there is no consequence for intertrial crossings (ITCs).

In AA2, mice receive a 0.2 sec foot-shock (0.3 mA) and white noise for each ITC. Therefore, in AA2, mice must passively avoid during the intertrial interval by inhibiting their tendency to shuttle between trials, termed intertrial crossings (ITCs). Thus, during AA2, mice perform both signaled active avoidance during the signaled avoidance interval (like in AA1) and unsignaled passive avoidance during the unsignaled intertrial interval.

In AA3, mice are subjected to a CS discrimination procedure in which they must respond differently to a CS1 (8 kHz tone at 85 dB) and a CS2 (4 kHz tone at 75 dB) presented randomly (half of the trials are CS1). Mice perform the basic signaled active avoidance to CS1 (like in AA1 and AA2), but also perform signaled passive avoidance to CS2, and ITCs are not punished. In AA3, if mice shuttle during the CS2 avoidance interval (7 sec), they receive a 0.5 sec foot-shock (0.3 mA) with white noise and the trial ends. If animals do not shuttle during the CS2

avoidance interval, the CS2 trial terminates at the end of the avoidance interval (i.e., successful signaled passive avoidance).

In AA4, three different CS's, CS1 (8 kHz tone at 85 dB), CS2 (10 kHz tone at 85 dB), and CS3 (12 kHz tone at 85 dB) signal a different avoidance interval duration of 4, 7, and 15 sec, respectively. Like in AA2, mice are punished for producing intertrial crossings. In AA4, mice adjust their response latencies according to the duration of the avoidance interval signaled by each CS.

In a modified version of AA1, AA2, and AA3, we introduced randomized presentations of CS1 (8 kHz), CS2 (4 kHz), and CS3 (12 kHz) at three different saliency levels (65, 75, and 85 dB), starting from the first AA1 session. In this design, CS1 predicted the aversive US and required an active avoidance response, while CS2 and CS3 were neutral—they predicted nothing. However, crossings during any CS turned off the tone, and crossings during CS1 also avoided the US. In AA2, ITCs were punished, and in AA3, mice were required to passively avoid (not cross) during CS2 to avoid the US while CS3 continued to be neutral.

There are three main variables representing task performance. The percentage of active avoidance responses (% avoids) represents the trials in which the animal actively avoided the US in response to the CS. The response latency (latency) represents the time (sec) at which the animal enters the safe compartment after the CS onset; avoidance latency is the response latency only for successful active avoidance trials (excluding escape trials). The number of crossings during the intertrial interval (ITCs) represents random shuttling due to locomotor activity in the AA1 and AA3 procedures, or failures to passively avoid in the AA2 procedure. The sound pressure level (SPL) of the auditory CS's were measured using a microphone (PCB Piezotronics 377C01) and amplifier (x100) connected to a custom LabVIEW application that samples the

stimulus within the shuttle cage as the microphone rotates driven by an actuator controlled by the application.

***Fiber photometry***

We employed a 2-channel excitation (465 and 405 nm) and 2-channel emission (525 and 430 nm for GCaMP6f and other emissions) fiber photometry system (Doric Lenses). Alternating light pulses were delivered at 100 Hz (per each 10 ms, 465 is on for 3 ms, and 2 ms later 405 is on for 3 ms). While monitoring the 525 nm emission channel, we set the 465 light pulses in the 20-60 µW power range and then the power of the 405 light pulses was adjusted (20-50 µW) to approximately match the response evoked by the 465 pulses. During recordings, the emission peak signals evoked by the 465 (GCaMP6f) and 405 (isobestic) light pulses were acquired at 5-20 kHz and measured at the end of each pulse. To calculate $F_o$, the measured peak emissions evoked by the 405 nm pulses were scaled to those evoked by the 465 pulses (F) using the slope of the linear fit. Finally, $F/F_o$ was calculated with the following formula: $(F-F_o)/F_o$ and converted to Z-scores. Due to the nature of the behavior studied, a swivel is essential. We employed a rotatory-assisted photometry system that has no light path interruptions (Doric Lenses). In addition, charcoal powder was mixed in the dental cement to assure that ambient light was not leaking into the implant and reaching the optical fiber; this was tested in each animal by comparing fluorescence signals in the dark versus normal cage illumination.

***Miniscope imaging***

We employed GRIN lenses (0.6mm diameter, 7.3mm length) and an nVista (Inscopix) recording system coupled with an electrical swivel. We added custom tungsten rods to the GRIN

lenses to maximize the stability of the recordings. During each session, we adjusted the focus plane to record the best neurons, which were assigned as neurons per session. We used Inscopix Data Processing Software (IDPS) to extract ROIs from the raw miniscope movies. Briefly, the movies were preprocessed with a spatial bandpass filter, which removes the low and high spatial frequency content from the movies minimizing out of plane neuropil fluorescence and allows visual identification of putative neurons. The movies were then motion corrected, using the initial frame as the global reference. Finally, neurons were manually outlined on the processed movie, and the F/F calcium activity was calculated from these ROIs. To assure stability during each recording session, the ROIs were visually verified from start to end for each video.

K-means clustering (scikit-learn) was performed on features extracted from F/F (z-score) or movement (speed) time series traces. These features included peak amplitudes, areas under the curve, and times to peak around specific events (e.g., turns, CS onset, or avoidance occurrence). Alternatively, clustering was also applied to principal component scores derived from the same traces, which were treated as an analog of spectral data for PCA.

***Optogenetics***

The implanted optical fibers were connected to patch cables using sleeves. A black aluminum cap covered the head implant and completely blocked any light exiting at the ferrule's junction. Furthermore, the experiments occurred in a brightly lit cage that made it difficult to detect any light escaping the implant. The other end of the patch cable was connected to a dual light swivel (Doric lenses) that was coupled to a green laser (520 nm; 100 mW) to activate Arch or a blue laser (450 nm; 80 mW) to activate ChR2. In experiments expressing Arch, Green light was applied continuously at different powers (3.5, 7, 15, 25 and 30 mW). In experiments with

ChR2 expression, blue light was delivered at constant power across different stimulation patterns, including continuous (Cont) and trains of 1-ms pulses at varying frequencies (2–100 Hz). Stimulation power was tested at three levels (~ 1, 3, and, more rarely, 6 mW) categorized as low or high depending on behavioral efficacy. For instance, if 3 mW reliably produced strong, maximal behavioral effects (e.g., rapid action onsets), 3 mW was designated as the high-power condition. Power is regularly measured by flashing the connecting patch cords onto a light sensor—with the sleeve on the ferrule.

During optogenetic experiments that involve avoidance procedures, we compared different trial types: CS, CS+Light, Light, NoCS, NoCS+Light, and Light US trials. *CS trials* were standard avoidance trials specific to each procedure, without optogenetic stimulation. *CS+Light trials* were identical to CS trials, except that optogenetic light was delivered simultaneously with the CS and the US during the avoid and escape intervals. *Light trials* were identical to CS+Light trials, but the CS was omitted to test whether optogenetic stimulation alone could substitute for the CS (cue). *NoCS trials* were catch trials with neither CS nor US, used to assess chance, baseline responses. *NoCS+Light trials* trials were identical to NoCS trials but included light stimulation to assess its effects in the absence of predictive cues or outcomes. These differed from Light trials in that they did not signal or result in a US. *Light US trials* were like CS trials, but the US was optogenetic stimulation. To perform within group repeated measures (RM) comparisons, the different trial types for a procedure were delivered randomly within the same session. In addition, the trials were compared between different groups, including No Opsin mice that did not express opsins but were subjected to the same trials including light delivery.

***Video tracking***

All mice in the study (open field or shuttle box) were continuously video tracked (30-100 FPS) in synchrony with the procedures and other measures. During open field experiments, mice are placed in a circular open field (10" diameter) that was illuminated from the bottom or in the standard shuttle box (16.1" x 6.5"). We automatically tracked head movements with two color markers attached to the head connector –one located over the nose and the other between the ears. The coordinates from these markers form a line (head midline) that serves to derive several instantaneous movement measures per frame (Zhou et al., 2023). Overall head movement was separated into *rotational* and *translational* components (unless otherwise indicated, overall head movement is presented for simplicity and brevity, but the different components were analyzed). Rotational movement was the angle formed by the head midline between succeeding video frames multiplied by the radius. Translational movement resulted from the sum of linear (forward vs backward) and sideways movements. *Linear* movement was the distance moved by the ears marker between succeeding frames multiplied by the cosine of the angle formed by the line between these succeeding ear points and the head midline. *Sideways* movement was calculated as linear movement, but the sine was used instead of the cosine. Pixel measures were converted to metric units using calibration and expressed as speed (cm/sec). We used the time series to extract window measurements around events (e.g., CS presentations). Measurements were obtained from single trial traces and/or from traces averaged over a session. In addition, we obtained the direction of the rotational movement with a *Head Angle* or *bias* measure, which was the accumulated change in angle of the head per frame (versus the previous frame) zeroed by the frame preceding the stimulus onset or event (this is equivalent to the rotational speed movement in degrees). The *time to peak* is when the *extrema* occurs versus event onset.

To detect spontaneous turns or movements from the head tracking, we applied a local maximum algorithm to the continuous head angle or speed measure, respectively. Every point is checked to determine if it is the maximum or minimum among the points in a range of 0.5 sec before and after the point. A change in angle of this point >10 degrees was a detected turn in the direction of the sign. We further sorted detected turns or movements based on the timing of previous detected events.

***Histology***

Mice were deeply anesthetized with an overdose of isoflurane. Upon losing all responsiveness to a strong tail pinch, the animals were decapitated, and the brains were rapidly extracted and placed in fixative. The brains were sectioned (100 µm sections) in the coronal or sagittal planes. Some sections were stained using Neuro-trace. All sections were mounted on slides, cover slipped with DAPI mounting media, and all the sections were imaged using a slide scanner (Leica Thunder). We used an APP we developed with OriginLab (Brain Atlas Analyzer) to align the sections with the Allen Brain Atlas Common Coordinate Framework (CCF) v3 (Wang et al., 2020). This reveals the location of probes and fluorophores versus the delimited atlas areas. We used it to determine the extent of the lesions by delimit DAPI or Neurotrace-stained sections of control, dtA and electrolytic lesion mice. We counted Neurotrace-stained neurons within STN using image stacks acquired with Leica Thunder using LAS X software.

## Figure Legends

**Figure 1**. Calcium imaging fiber photometry reveals that STN glutamatergic neurons activate during spontaneous exploratory movement.

***A***, Parasagittal section showing the optical fiber tract reaching STN and GCaMP7f fluorescence expressed in glutamatergic neurons around the fiber ending. The section was aligned with the Allen brain atlas. ZI, zona incerta; SNr, substantia nigra pars reticulata; STN, subthalamic nucleus.

**B**, Cross-correlation between movement and STN $F/F_o$ for the overall (black traces), rotational (red) and translational (cyan) components (upper panel). Per session (dots) and mean±SEM (rectangle) linear fit (correlation, r) between overall movement and STN $F/F_o$, including the rotational and translational components (lower panel). The lighter dots show the linear fits after scrambling one of the variables (lower panel, shuffled).

***C***, $F/F_o$ calcium imaging time extracted around detected spontaneous movements. Time zero represents the peak of the movement. The upper traces show $F/F_o$ mean±SEM of all movement peaks (black), those that had no detected peaks 3 sec prior (red), and peaks taken at a fixed interval >5 sec (cyan). The lower traces show the corresponding movement speed for the selected peaks. All traces in the paper are mean±SEM.

**Figure 2**. STN glutamatergic neurons code the direction of spontaneous contraversive exploratory turning movements.

***A***, $F/F_o$ calcium imaging, overall movement, rotational movement, and angle of turning direction for detected movements classified by the turning direction (ipsiversive and contraversive; red and cyan) versus the side of the recording (implanted optical fiber). At time zero, the animals spontaneously turn their head in the indicated direction. The columns show all turns (left), those that included no turn peaks 3 sec prior (middle), and peaks selected at a fixed interval >5 sec (right). Note that the speed of the movements was similar in both directions.

***B***, Population measures (area of traces 3 sec around the detected peaks) of $F/F_o$ and movement (overall, rotational, and translational) for the different classified peaks. Asterisks denote significant differences ($p<0.05$) between ipsiversive and contraversive movements.

**Figure 3**. A subgroup of STN glutamatergic neurons code contraversive movements.

***A***, Parasagittal section showing a miniscope GRIN lens tract reaching STN and GCaMP7f fluorescence expressed in STN glutamatergic neurons. The section was aligned with the Allen brain atlas. The red inset shows a FOV of imaged cells during a recording session. ZI, zona incerta; STN, subthalamic nucleus.

***B,*** Classification of STN glutamatergic neurons during spontaneous movement onsets with k-means reveals three classes (mean±SEM). The top traces show F/F calcium imaging, and the bottom traces show the movement onset. Class 1 neurons activated weakly during movement onset. Class 2 neurons were inhibited while Class 3 neurons activated sharply during movement onset.

***C***, Classification of STN glutamatergic neurons during spontaneous turning movements with k-means reveals three classes (mean±SEM). The top traces show F/F calcium imaging, and the bottom traces show angle of turning direction for detected movements separated by class. The left panels show the activation difference (bias) between contraversive-ipsiversive directions used to classify the cells. The middle and right panels show the corresponding contraversive and ipsiversive movements. Class 1 neurons did not activate during turns and did not code turn direction. Class 2 neurons showed stronger activation in the ipsiversive direction. Class 3 neurons activated more strongly than Class 2 in the contraversive direction.

***D***, Population comparison of F/F Peak amplitude bias (difference between contravesive-ipsiversive direction) for the three classes of neurons. Asterisks denote significant differences ($p<0.05$) between both directions. The k-means clusters of the three cell classes from C are shown on the top panel.

***E***, Unilateral optogenetic STN excitation drives an ipsiversive head orienting bias. Light patterns (2 sec at different frequencies) are delivered randomly as mice explore an arena. The top left panel shows head orienting angle change from the onset of the light. The bottom left panel shows the movement speed. Note the strong ipsiversive bias during 40-66 Hz STN excitation. The right panels show population data comparing Opsin mice expressing ChR2 in STN neurons with No Opsin mice. Asterisks denote significant differences ($p<0.05$) between Opsin and No Opsin mice.

**Figure 4**. STN glutamatergic neurons discharge to auditory tones in association with movement.

***A***, Example $F/F_o$ calcium imaging and movement traces (mean±SEM) evoked from STN neurons by auditory tones (1 sec) of different saliency. The tones vary in frequency (4-16 kHz) and SPL (low and high dB).

***B***, Area of $F/F_o$, overall movement, and movement components (rotational and translational) measured during a time window (0-2 s) after tone onset.

**Figure 5**. STN glutamatergic neuron activation in the context of signaled active avoidance.

***A***, Arrangement of the shuttle box used during signaled avoidance tasks.

***B***, Behavioral performance during the four different avoidance procedures (AA1-4) showing the percentage of active avoids (black circles), avoidance latency (orange triangles), and ITCs (cyan bars).

***C***, $F/F_o$ and overall movement traces from CS onset for AA1, AA2 and AA3 (CS1 and CS2) procedures per trials classified as avoids (left) or escapes (right) of CS-evoked orienting responses measured by tracking overall head speed.

***D,*** Same as C from response occurrence.

***E***, Population measures of F/Fo and speed for avoids and escapes during AA1, AA2 and AA3 (CS1). Asterisks denote significant differences ($p<0.05$) between avoids and escapes.

**Figure 6**. STN glutamatergic neurons track the avoidance and escape movement.

***A***, $F/F_o$ and overall movement traces from CS onset (left) and response occurrence (right) for avoids during the AA4 procedure, which include three CSs that signal avoidance intervals of different durations.

***B***, Population measures (-3 to 3 sec area, mean ± SEM) from response occurrence. Asterisks denote significant differences vs other stimuli.

***C***, $F/F_o$ and overall movement traces from US onset for escapes during the unsignaled US procedure, which includes the US, or each of its components delivered alone (foot-shock and white noise).

***D***, Population measures (0 to 5 sec area, mean ± SEM) for the data in C. Asterisks denote significant differences ($p<0.05$) between a condition and the other conditions.

**Figure 7**. Different classes of STN glutamatergic neurons during signaled active avoidance.

***A***, k-means clustering of the speed time series from CS onset (gray panel) revealed three distinct classes of signaled active avoidance responses. Class 1 avoids start early after CS onset while Class 2 and Class 3 avoids start later reflecting delayed responding. The top panel shows the F/F activation of all the recorded STN neurons during each class of avoids. Class 1 avoids were associated with little STN neuron activation followed by Class 2 avoids, while Class 3 avoids were associated with strong STN activation.

***B,*** k-means clustering of the F/F time series within each Class of avoids in A revealed three classes (types: a-c) of neurons. Type a (1-3a) neurons showed little STN activation. Type b (1-3b) neurons activated during all avoids classes but showed inhibition at CS onset prior to Class 1 avoid. Type c (1-3c) showed stronger activation than the other types but activated most sharply during Class 3 avoids, which have the longest response delays.

***C***,***D***, The same data shown in A and B are displayed from avoidance response occurrence (instead of CS onset).

***E***, Population comparison of F/F parameters for the classes of avoids and neuron types shown in A-D. Asterisks denote significant differences ($p<0.05$) between the noted avoid classes or neuron types. The panels show baseline (prior to CS onset; left panel), orienting and avoidance responses from CS onset (middle panels) or from avoid occurrence (right panel).

***F***, Same as E for the corresponding movement (speed) parameters (baseline corrected areas of speed traces).

**Figure 8**. Optogenetic activation of ChR2-expressing STN glutamatergic neurons drives signaled active avoidance and can substitute for the natural CS.

***A***, Parasagittal section showing the optical fiber tract reaching STN and ChR2 fluorescence expressed in glutamatergic neurons. The section was aligned with the Allen brain atlas.

***B,*** Effects of blue light patterns on signaled active avoidance. Blue circles show the effect of CS+Light trials (filled blue circles) compared to control CS trials (open blue circle) and catch NoCS trials (open blue squares). Note the shortening of the latency for higher frequencies including Cont light. The cyan triangles show the results for equivalent Light trials, where the CS is excluded, and the light serves as the CS. Light trials at low frequencies are ineffective at driving avoids.

***C***, Traces of the overall speed during AA1 for CS trials and CS+Light trials for different light patterns. The trials are aligned by CS onset (left and middle panels), which reveals the orienting response evoked by the CS followed by the avoidance action, or from avoid occurrence (right panel), which reveals the peak speed as the mice cross between compartments.

***D***, Population measures of peak speed and time to peak speed for CS and CS+Light trials from CS onset, for the orienting response and the avoidance response peaks from CS onset (left and middle panels). The right panel compares the peak speed measured from the avoid occurrence. CS+Light trials data are combined according to the light pattern into low frequency (2-20 Hz) or high frequency (>20 Hz and Cont). Asterisks denote significant differences ($p<0.05$) between CS trials and CS+Light trials.

**E,** and **F**, Same as C and D but compares CS trials and Light trials. This tests the ability of the light alone to serve as CS in the absence of the natural tone.

**Figure 9**. Optogenetic activation of ChR2-expressing STN glutamatergic neurons drives crossings in naïve mice, suppresses the development of caution, and is incompatible with passive avoidance.

***A,*** Effects of patterns of blue light applied in the STN of naïve mice where the light does not predict the US (NoCS+Light trials, blue circles). This was followed by the addition of the US in regular Light trials (red triangles). Note that STN excitation in naïve mice drives a high rate of crossings.

***B***, Development of caution between AA1 and AA2 (by punishing ITCs) and reflected in the avoidance latency is suppressed by STN excitation in STN-ChR2 mice compared to No Opsin controls. The blue circles show AA1 sessions followed by red squares showing AA2 sessions in the same mice for STN-ChR2 and No Opsin mice. Note the abolishment of ITCs during AA2 and the shift of the latency longer only in No Opsin mice. Asterisks denote significant differences ($p<0.05$) between AA1 (blue) and AA2 (red).

***C,*** Traces of overall speed during AA1 and AA2 for the data shown in B. Note the characteristic changes in No Opsin mice are blunted by STN excitation in STN-ChR2 mice. This includes the rightward shift of the speed from CS onset, and the larger peak speed from response occurrence during AA2 compared to AA1.

***D,*** STN excitation blocks signaled passive avoidance. In AA3, CS1 signals the animal to actively avoid, while CS2 signals the animal to passively avoid by not crossing. In addition, we tested CS2+Light trials and NoCS+Light trials (40-60 Hz light). STN excitation virtually abolished passive avoids to CS2 so that mice crossed despite being punished. Moreover, mice also crossed during NoCS trials when the light was delivered.

***E,*** Traces of overall speed during AA3 for the data in D.

***F***, Population measurements of peak speed for the data in E. Asterisks denote significant differences ($p<0.05$) between CS2 and the other conditions.

**Figure 10.** Optogenetic STN excitation is not aversive.

***A***, Signaled active avoidance procedures where the normal aversive US is substituted for STN optogenetic excitation that drives fast escape responses. Mice were subjected to AA1, followed by AA2 and then AA3 using 3 different CS's. During AA1, CS1 predicts STN stimulation, while CS2 and CS3 predict nil. During AA2, ITCs are punished with STN stimulation. During AA3, mice must passively avoid by not responding when CS2 is presented, so active avoids driven by CS2 are errors. The bars show side by side the results for Opsin (black, red, cyan) and No Opsin mice (gray) in the same procedures. Asterisks denote significant differences ($p<0.05$) between Opsin vs No Opsin mice.

***B***, The mice in A are subjected to the same procedures using the normal aversive US. Asterisks denote significant differences ($p<0.05$) between Opsin vs No Opsin mice.

**Figure 11.** Optogenetic inhibition of STN glutamatergic neurons impairs signaled avoidance.

***A,*** Effect of Cont green light delivered at different powers on AA1 (green circles), AA2 (red circles) and AA3 (right panel) in mice expressing eArch3.0 in STN glutamatergic neurons. Note the strong abolishment of active avoidance responses in CS+Light trials for AA1, AA2, and AA3-CS1. In contrast, passive avoids during AA3-CS2 were not impaired.

***B,*** Traces of overall movement (speed) during AA1, AA2 and AA3 for CS trials and CS+Light trials combined for different light powers. The trials are aligned by CS onset, which reveals the orienting response evoked by the CS followed by the ensuing avoid action.

***C,*** Population data of peak speed from CS onset for orienting and avoidance responses during AA1, AA2, and AA3. Asterisks denote significant differences ($p<0.05$) between CS vs CS+Light.

**Figure 12**. Lesions of STN glutamatergic neurons impair signaled avoidance learning and performance.

***A***, Coronal Neurotrace (green) stained section of a Vglut2-Cre mouse injected with a Cre-dependent AAV-dtA in the STN to kill glutamatergic neurons. We counted the number of cells in the STN in controls and lesion mice. There was a significant reduction ($p<0.05$) in the number of STN neurons in the lesion mice.

***B***, Behavioral performance during learning of AA1, followed by AA2 and AA3 procedures showing the percentage of active avoids (upper), avoid latency (middle), and ITCs (lower) for control and lesion mice. The AA3 procedure shows CS1 and CS2 trials for the same sessions. Active avoids during AA3-CS2 trials are errors, as the mice must passively avoid during CS2. Lesion mice were significantly impaired compared to control mice.

***C***, Movement (speed) from CS onset (left) and from avoid occurrence (right) during AA1 and AA2 procedures for control and lesion mice. The lesion had significant effects on movement measured from CS onset or avoid occurrence.

***D,*** Same as ***C*** for AA3.

***E***, Population measures of orienting, avoidance, and escape responses from CS onset (left) and from response occurrence (right) for overall movement. Asterisks denote significant differences ($p<0.05$) between Control and Lesion.

***F***, Bilateral electrolytic lesions targeting the STN.

***G***, Effect of bilateral electrolytic STN lesions on behavioral performance in a repeated measures design. The plot shows the percentage of active avoids (filled black circles), avoid latency (open orange squares), and ITCs (cyan bars). Mice were trained in AA1 prior to the lesion and then placed back in AA1, followed by AA2 and AA3. The lesion decreased the percentage of active avoids compared to AA1. During AA2, mice learned to suppress their ITCs. During AA3, lesion mice were impaired in active avoids during CS1 but passively avoided during CS2.

**Figure 13**. Optogenetic activation of STN glutamatergic pathways to the midbrain, not to GPe, mediate the effects of excitation within STN.

***A,*** Schematic of optical fiber locations for the midbrain targeting midbrain tegmentum (SNr and mRt combined) and GPe groups to target fibers originating in STN.

***B***, Effects of blue light patterns (CS+Light) applied in the Midbrain (filled triangles) or in the GPe (filled red circles) of STN-ChR2 mice on signaled active avoidance. A group of No Opsin mice are also included (filled back squares). Both optogenetic groups activated in the Midbrain and GPe received low and higher power light, but this is shown separately for the midbrain group as there was no effect of the light in the GPe group. Note that the effects in the Midbrain group occur for high frequency trains 20-100 Hz but not Cont light, which is consistent with the effective sustained activation of fibers with pulsed trains, not with Cont light.

***C***, Development of cautious responding from AA1 to AA2 (induced by punishing ITCs) is reflected in increased avoidance latencies and is suppressed by excitation of STN fibers in the midbrain, but not by excitation of STN fibers in the GPe or in No Opsin controls. Note the abolishment of ITCs during AA2 across groups, and the latency shift toward longer response times observed only in GPe and No Opsin mice.

***D,*** Signaled passive avoidance is blocked when STN fibers to midbrain are excited but not those to GPe or in No Opsin mice. In AA3, CS1 signals the animal to actively avoid (open black squares), while CS2 signals the animal to passively avoid by not crossing (open red circles). Application of CS2+Light (filled red circles) and NoCS+Light (filled gray triangles) trials (40-60 Hz light) in Midbrain but not in GPe virtually abolished passive avoids to CS2 and induced crossings in response to the light alone.

***E,*** Ability of STN fiber excitation in the Midbrain or GPe to serve as a CS assessed by comparing CS and Light trials. Only excitation of STN fibers in the midbrain was sufficient to drive active avoidance responses, whereas stimulation of STN fibers in the GPe was ineffective and comparable to responses in No Opsin controls.

**Figure 14**. Optogenetic inhibition of STN glutamatergic fibers in Midbrain impairs signaled avoidance.

***A,*** Effect of Cont green light delivered at different powers (Lo or Hi) on AA1, AA2 and AA3 in mice expressing eArch3.0 in STN glutamatergic neurons. Note the strong abolishment of active

avoidance responses in CS+Light trials for AA1, AA2, and AA3-CS1. In contrast, passive avoids during AA3-CS2 were not impaired. The light had no effect in No Opsin mice (filled gray squares).

***B,*** Traces of overall movement (speed) during AA1, AA2 and AA3 for CS trials and CS+Light trials combined for different light powers. The trials are aligned by CS onset, which reveals the orienting response evoked by the CS followed by the ensuing avoid action.

***C,*** Population data of peak speed from CS onset for orienting and avoidance responses during AA1, AA2, and AA3. Asterisks denote significant differences ($p<0.05$) between CS vs CS+Light.

**References**


Albin RL, Young AB, Penney JB (1989) The functional anatomy of basal ganglia disorders. Trends Neurosci 12:366-375.

Aristieta A, Barresi M, Azizpour Lindi S, Barrière G, Courtand G, de la Crompe B, Guilhemsang L, Gauthier S, Fioramonti S, Baufreton J, Mallet NP (2021) A Disynaptic Circuit in the Globus Pallidus Controls Locomotion Inhibition. Current Biology 31:707-721.e707.

Aron AR (2011) From Reactive to Proactive and Selective Control: Developing a Richer Model for Stopping Inappropriate Responses. Biological Psychiatry 69:e55-e68.

Bevan MD (2021) Motor Control: A Basal Ganglia Feedback Circuit for Action Suppression. Curr Biol 31:R191-r193.

Bogacz R, Wagenmakers EJ, Forstmann BU, Nieuwenhuis S (2010) The neural basis of the speed-accuracy tradeoff. Trends Neurosci 33:10-16.

Bonnevie T, Zaghloul KA (2018) The Subthalamic Nucleus: Unravelling New Roles and Mechanisms in the Control of Action. The Neuroscientist 25:48-64.

Callahan JW, Morales JC, Atherton JF, Wang D, Kostic S, Bevan MD (2024) Movement-related increases in subthalamic activity optimize locomotion. Cell reports 43:114495.

Canteras NS, Shammah-Lagnado SJ, Silva BA, Ricardo JA (1990) Afferent connections of the subthalamic nucleus: a combined retrograde and anterograde horseradish peroxidase study in the rat. Brain Res 513:43-59.

Castro-Alamancos MA (2022) A System to Easily Manage Metadata in Biomedical Research Labs Based on Open-source Software. Bio Protoc 12:e4404.

Cavanagh JF, Sanguinetti JL, Allen JJ, Sherman SJ, Frank MJ (2014) The subthalamic nucleus contributes to post-error slowing. J Cogn Neurosci 26:2637-2644.

Cavanagh JF, Wiecki TV, Cohen MX, Figueroa CM, Samanta J, Sherman SJ, Frank MJ (2011) Subthalamic nucleus stimulation reverses mediofrontal influence over decision threshold. Nature Neuroscience 14:1462-1467.

Chen TW, Wardill TJ, Sun Y, Pulver SR, Renninger SL, Baohan A, Schreiter ER, Kerr RA, Orger MB, Jayaraman V, Looger LL, Svoboda K, Kim DS (2013) Ultrasensitive fluorescent proteins for imaging neuronal activity. Nature 499:295-300.

DeLong MR (1990) Primate models of movement disorders of basal ganglia origin. Trends Neurosci 13:281-285.

Fan JP, Zhang X, Han Y, Ji Y, Gu WX, Wu HC, Zhou C, Xiao C (2023) Subthalamic neurons interact with nigral dopaminergic neurons to regulate movement in mice. Acta physiologica (Oxford, England) 237:e13917.

Fife KH, Gutierrez-Reed NA, Zell V, Bailly J, Lewis CM, Aron AR, Hnasko TS (2017) Causal role for the subthalamic nucleus in interrupting behavior. eLife 6:e27689.

Frank MJ, Samanta J, Moustafa AA, Sherman SJ (2007) Hold Your Horses: Impulsivity, Deep Brain Stimulation, and Medication in Parkinsonism. Science 318:1309-1312.

Friedman AD, Yin HH (2023) Selective Activation of Subthalamic Nucleus Output Quantitatively Scales Movements. J Neurosci 43:7967-7981.

Gerfen CR, Wilson CJ (1996) Chapter II The basal ganglia. In: Handbook of chemical neuroanatomy, pp 371-468: Elsevier.

Gittis AH, Sillitoe RV (2024) Circuit-Specific Deep Brain Stimulation Provides Insights into Movement Control. Annu Rev Neurosci 47:63-83.

Gold JI, Shadlen MN (2007) The neural basis of decision making. Annu Rev Neurosci 30:535-574.

Guillaumin A, Serra GP, Georges F, Wallén-Mackenzie Å (2021) Experimental investigation into the role of the subthalamic nucleus (STN) in motor control using optogenetics in mice. Brain Research 1755:147226.
Guitart-Masip M, Huys QJM, Fuentemilla L, Dayan P, Duzel E, Dolan RJ (2012) Go and no-go learning in reward and punishment: Interactions between affect and effect. NeuroImage 62:154-166.
Haber SN, Yendiki A, Jbabdi S (2021) Four Deep Brain Stimulation Targets for Obsessive-Compulsive Disorder: Are They Different? Biol Psychiatry 90:667-677.
Heitz RP, Schall JD (2012) Neural mechanisms of speed-accuracy tradeoff. Neuron 76:616-628.
Herz DM, Frank MJ, Tan H, Groppa S (2024) Subthalamic control of impulsive actions: insights from deep brain stimulation in Parkinson's disease. Brain 147:3651-3664.
Herz DM, Little S, Pedrosa DJ, Tinkhauser G, Cheeran B, Foltynie T, Bogacz R, Brown P (2018) Mechanisms Underlying Decision-Making as Revealed by Deep-Brain Stimulation in Patients with Parkinson's Disease. Curr Biol 28:1169-1178.e1166.
Hormigo S, Vega-Flores G, Castro-Alamancos MA (2016) Basal Ganglia Output Controls Active Avoidance Behavior. J Neurosci 36:10274-10284.
Hormigo S, Zhou J, Castro-Alamancos MA (2020) Zona Incerta GABAergic Output Controls a Signaled Locomotor Action in the Midbrain Tegmentum. eNeuro 7.
Hormigo S, Zhou J, Castro-Alamancos MA (2021a) Bidirectional control of orienting behavior by the substantia nigra pars reticulata: distinct significance of head and whisker movements. eNeuro.
Hormigo S, Vega-Flores G, Rovira V, Castro-Alamancos MA (2019) Circuits That Mediate Expression of Signaled Active Avoidance Converge in the Pedunculopontine Tegmentum. J Neurosci 39:4576-4594.
Hormigo S, Shanmugasundaram B, Zhou J, Castro-Alamancos MA (2021b) A Signaled Locomotor Avoidance Action Is Fully Represented in the Neural Activity of the Midbrain Tegmentum. J Neurosci 41:4262-4275.
Hormigo S, Zhou J, Chabbert D, Shanmugasundaram B, Castro-Alamancos MA (2021c) Basal Ganglia Output Has a Permissive Non-Driving Role in a Signaled Locomotor Action Mediated by the Midbrain. J Neurosci 41:1529-1552.
Hormigo S, Zhou J, Chabbert D, Sajid S, Busel N, Castro-Alamancos M (2023) Zona incerta distributes a broad movement signal that modulates behavior. Elife 12:RP89366.
Isoda M, Hikosaka O (2008) Role for Subthalamic Nucleus Neurons in Switching from Automatic to Controlled Eye Movement. The Journal of Neuroscience 28:7209.
Kita H, Kitai ST (1987) Efferent projections of the subthalamic nucleus in the rat: light and electron microscopic analysis with the PHA-L method. J Comp Neurol 260:435-452.
Kita T, Kita H (2011) Cholinergic and non-cholinergic mesopontine tegmental neurons projecting to the subthalamic nucleus in the rat. Eur J Neurosci 33:433-443.
Klaus A, Alves da Silva J, Costa RM (2019) What, If, and When to Move: Basal Ganglia Circuits and Self-Paced Action Initiation. Annu Rev Neurosci 42:459-483.
Limousin P, Pollak P, Benazzouz A, Hoffmann D, Le Bas JF, Perret JE, Benabid AL, Broussolle E (1995) Effect on parkinsonian signs and symptoms of bilateral subthalamic nucleus stimulation. The Lancet 345:91-95.
Malgady JM, Baez A, Hobel ZB, Jimenez K, Goldfried J, Prager EM, Wilking JA, Zhang Q, Feng G, Plotkin JL (2023) Pathway-specific alterations in striatal excitability and cholinergic modulation in a SAPAP3 mouse model of compulsive motor behavior. Cell reports 42:113384.
Mallet L et al. (2008) Subthalamic nucleus stimulation in severe obsessive-compulsive disorder. N Engl J Med 359:2121-2134.
Mallet N, Schmidt R, Leventhal D, Chen F, Amer N, Boraud T, Berke Joshua D (2016) Arkypallidal Cells Send a Stop Signal to Striatum. Neuron 89:308-316.

Nambu A, Tokuno H, Takada M (2002) Functional significance of the cortico–subthalamo–pallidal 'hyperdirect' pathway. Neuroscience Research 43:111-117.
Pagnier GJ, Asaad WF, Frank MJ (2024) Double dissociation of dopamine and subthalamic nucleus stimulation on effortful cost/benefit decision making. Current Biology 34:655-660.e653.
Parolari L, Schneeberger M, Heintz N, Friedman JM (2021) Functional analysis of distinct populations of subthalamic nucleus neurons on Parkinson's disease and OCD-like behaviors in mice. Mol Psychiatry 26:7029-7046.
Pisanello M, Pisano F, Hyun M, Maglie E, Balena A, De Vittorio M, Sabatini BL, Pisanello F (2019) The Three-Dimensional Signal Collection Field for Fiber Photometry in Brain Tissue. Front Neurosci 13:82.
Prasad AA, Wallen-Mackenzie A (2024) Architecture of the subthalamic nucleus. Commun Biol 7:78.
Ratcliff R, Frank MJ (2012) Reinforcement-based decision making in corticostriatal circuits: mutual constraints by neurocomputational and diffusion models. Neural Comput 24:1186-1229.
Schmidt R, Leventhal DK, Mallet N, Chen F, Berke JD (2013) Canceling actions involves a race between basal ganglia pathways. Nat Neurosci 16:1118-1124.
Serra GP, Guillaumin A, Vlcek B, Delgado-Zabalza L, Ricci A, Rubino E, Dumas S, Baufreton J, Georges F, Wallén-Mackenzie Å (2023) A role for the subthalamic nucleus in aversive learning. Cell reports 42:113328.
Smith PL, Ratcliff R (2004) Psychology and neurobiology of simple decisions. Trends Neurosci 27:161-168.
Smith Y, Bevan MD, Shink E, Bolam JP (1998) Microcircuitry of the direct and indirect pathways of the basal ganglia. Neuroscience 86:353-387.
Thorndike EL (1898) Animal intelligence: An experimental study of the associative processes in animals. The Psychological Review: Monograph Supplements 2:i-109.
Valenstein ES, Valenstein T (1964) INTERACTION OF POSITIVE AND NEGATIVE REINFORCING NEURAL SYSTEMS. Science 145:1456-1458.
van Maanen L, Brown SD, Eichele T, Wagenmakers EJ, Ho T, Serences J, Forstmann BU (2011) Neural correlates of trial-to-trial fluctuations in response caution. J Neurosci 31:17488-17495.
Wang Q et al. (2020) The Allen Mouse Brain Common Coordinate Framework: A 3D Reference Atlas. Cell 181:936-953 e920.
Watson GDR, Hughes RN, Petter EA, Fallon IP, Kim N, Severino FPU, Yin HH (2021) Thalamic projections to the subthalamic nucleus contribute to movement initiation and rescue of parkinsonian symptoms. Sci Adv 7.
Wilson CJ, Bevan MD (2011) Intrinsic dynamics and synaptic inputs control the activity patterns of subthalamic nucleus neurons in health and in Parkinson's disease. Neuroscience 198:54-68.
Xie C, Power J, Prasad AA (2022) Bidirectional Optogenetic Modulation of the Subthalamic Nucleus in a Rodent Model of Parkinson's Disease. Front Neurosci 16:848821.
Yee DM, Leng X, Shenhav A, Braver TS (2022) Aversive motivation and cognitive control. Neuroscience & Biobehavioral Reviews 133:104493.
Zhou J, Hormigo S, Sajid MS, Castro-Alamancos MA (2022) Caution Influences Avoidance and Approach Behaviors Differently. J Neurosci 42:5899-5915.
Zhou J, Hormigo S, Busel N, Castro-Alamancos MA (2023) The Orienting Reflex Reveals Behavioral States Set by Demanding Contexts: Role of the Superior Colliculus. J Neurosci 43:1778-1796.
Zhou J, Hormigo S, Sajid MS, Castro-Alamancos MA (2024) Role of the Nucleus Accumbens in Signaled Avoidance Actions. eNeuro 11.

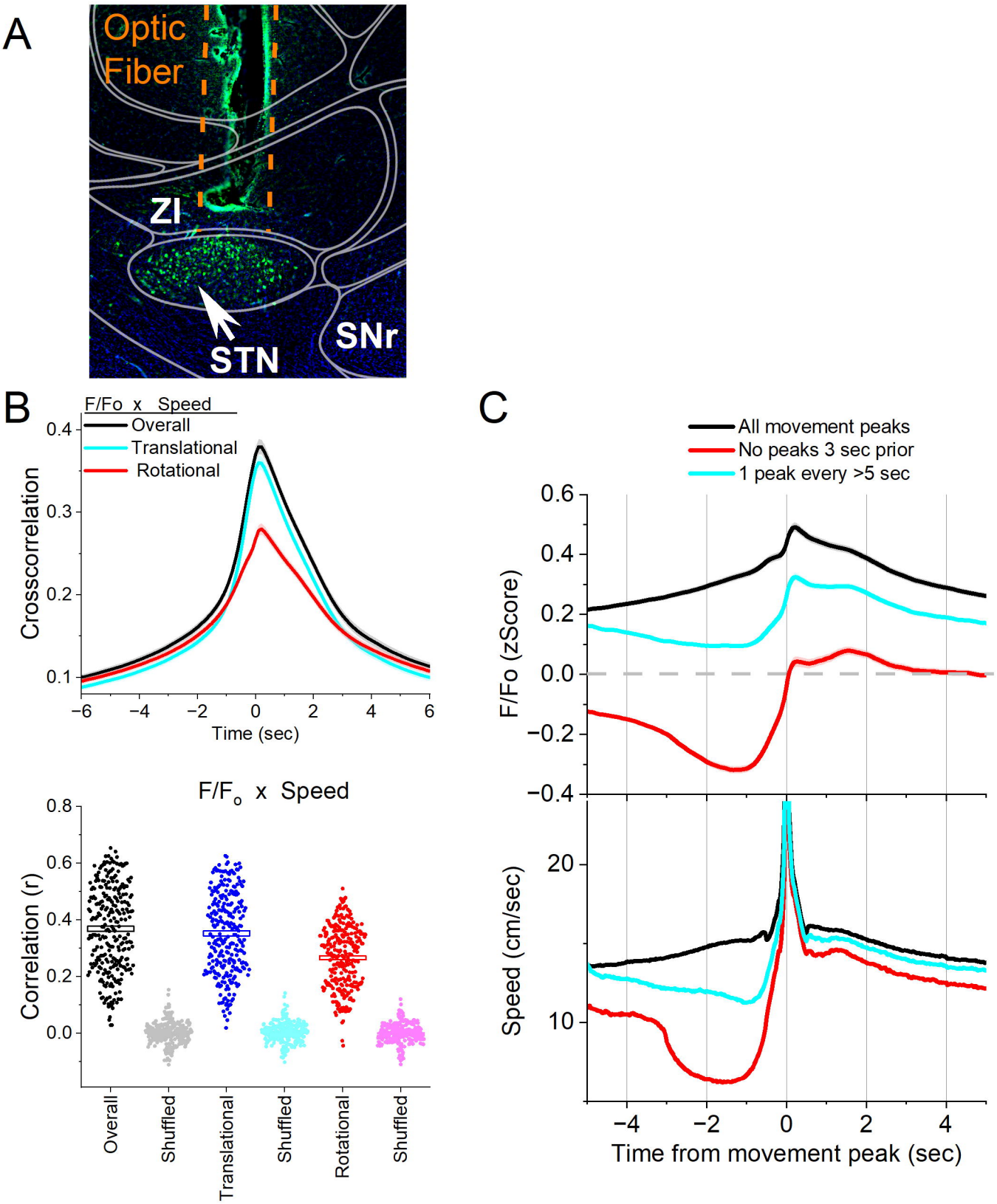
A
Optic
Fiber
ZI
STN
SNr
B
F/Fo x Speed
Overall
Translational
Rotational
Crosscorrelation
0.4
0.3
0.2
0.1
−6
−4
−2
0
2
4
6
Time (sec)
F/F$_o$ x Speed
Correlation (r)
0.8
0.6
0.4
0.2
0.0
Overall
Shuffled
Translational
Shuffled
Rotational
Shuffled
C
All movement peaks
No peaks 3 sec prior
1 peak every >5 sec
F/Fo (zScore)
0.6
0.4
0.2
0.0
−0.2
−0.4
Speed (cm/sec)
20
10
−4
−2
0
2
4
Time from movement peak (sec)

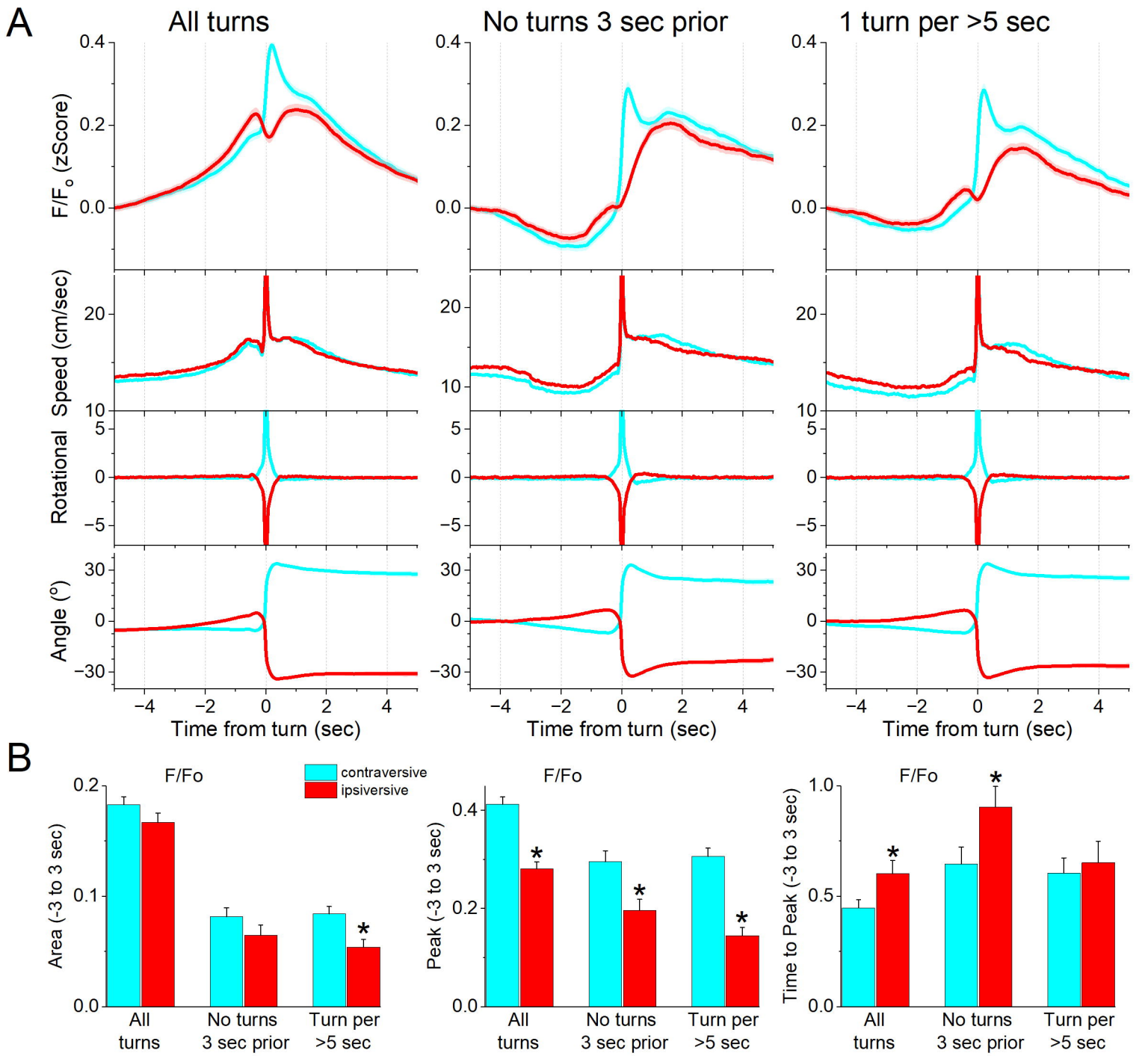
A
All turns
No turns 3 sec prior
1 turn per >5 sec
F/F$_o$ (zScore)
Speed (cm/sec)
Rotational
Angle (°)
Time from turn (sec)
B
F/Fo
contraversive
ipsiversive
Area (-3 to 3 sec)
Peak (-3 to 3 sec)
Time to Peak (-3 to 3 sec)
All turns
No turns 3 sec prior
Turn per >5 sec

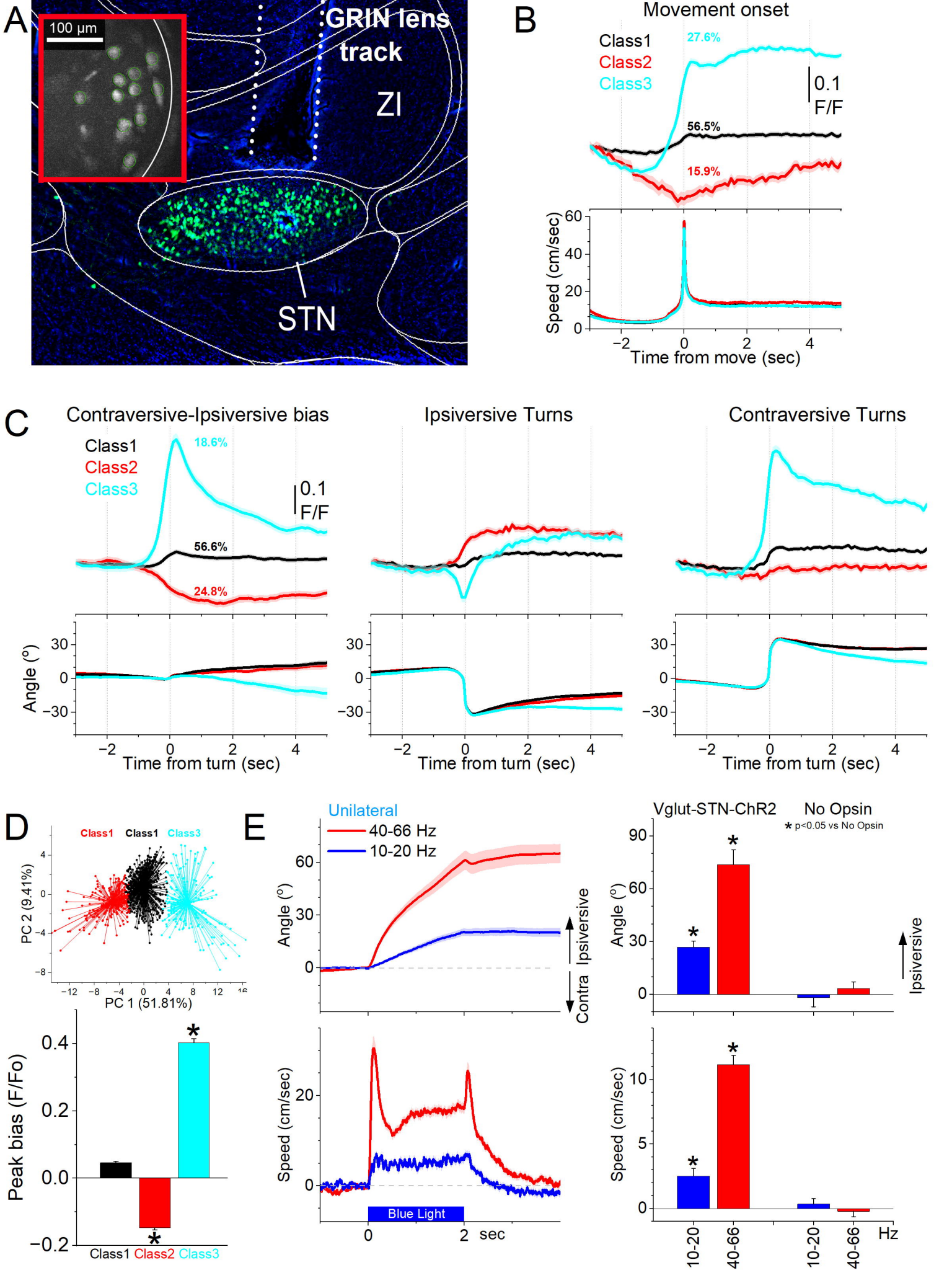
A
100 µm
GRIN lens track
ZI
STN
B
Movement onset
Class1
Class2
Class3
27.6%
56.5%
15.9%
0.1 F/F
Speed (cm/sec)
Time from move (sec)
C
Contraversive-Ipsiversive bias
Ipsiversive Turns
Contraversive Turns
Class1
Class2
Class3
18.6%
56.6%
24.8%
0.1 F/F
Angle (°)
Time from turn (sec)
D
Class1
Class1
Class3
PC 2 (9.41%)
PC 1 (51.81%)
Peak bias (F/Fo)
Class1 Class2 Class3
E
Unilateral
40-66 Hz
10-20 Hz
Angle (°)
Ipsiversive
Contra
Speed (cm/sec)
Blue Light
sec
Vglut-STN-ChR2
No Opsin
* p<0.05 vs No Opsin
Hz
10-20
40-66
10-20
40-66

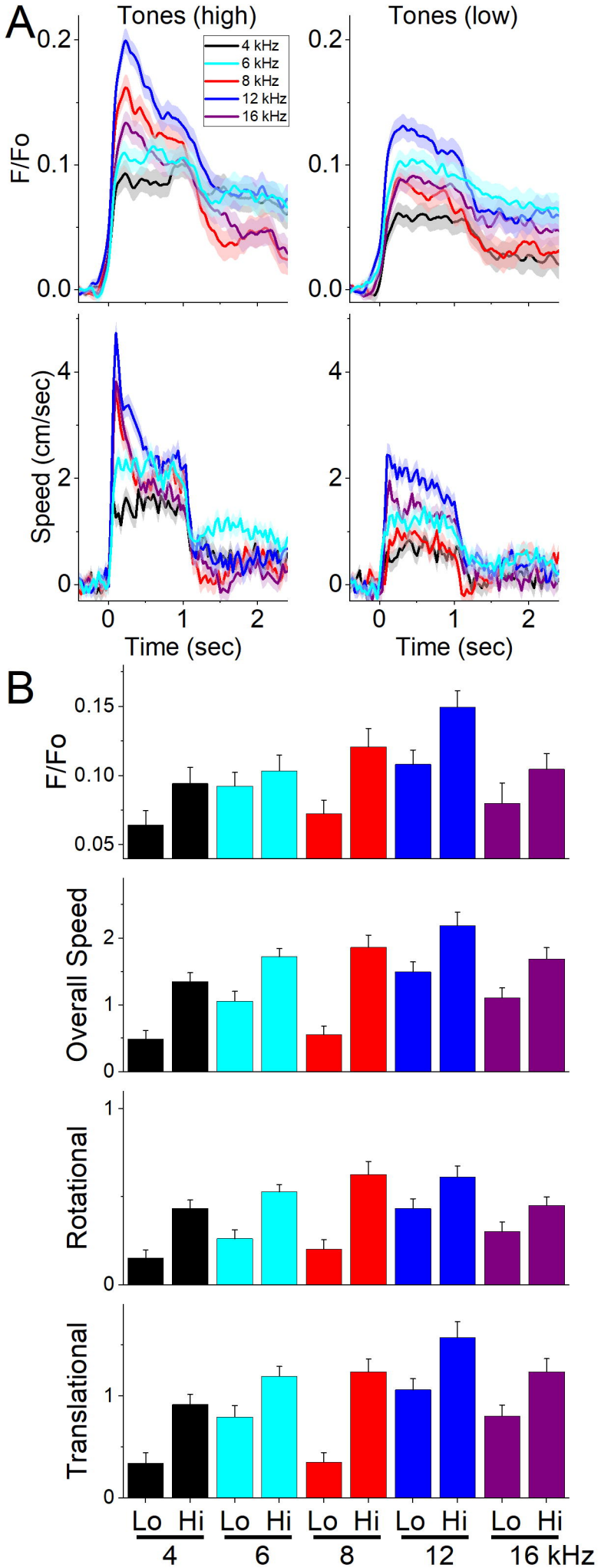
A
Tones (high)
Tones (low)
4 kHz
6 kHz
8 kHz
12 kHz
16 kHz
F/Fo
0.2
0.1
0.0
Speed (cm/sec)
4
2
0
0
1
2
Time (sec)
B
F/Fo
0.15
0.10
0.05
Overall Speed
2
1
0
Rotational
1
0
Translational
1
0
Lo Hi Lo Hi Lo Hi Lo Hi Lo Hi
4
6
8
12
16 kHz

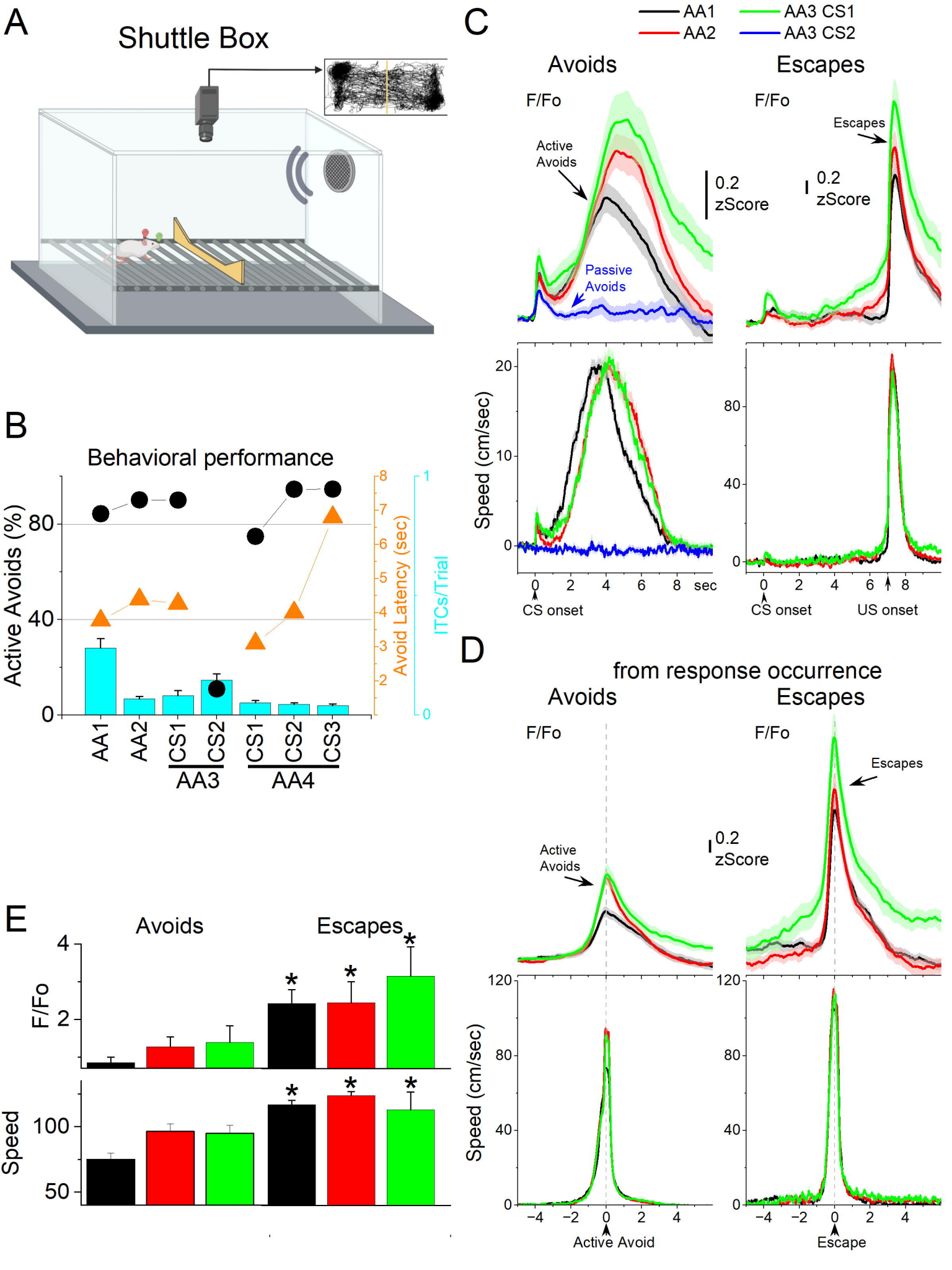
A
Shuttle Box
B
Behavioral performance
Active Avoids (%)
Avoid Latency (sec)
ITCs/Trial
AA1
AA2
CS1
CS2
CS1
CS2
CS3
AA3
AA4
C
AA1
AA2
AA3 CS1
AA3 CS2
Avoids
Escapes
F/Fo
Active Avoids
Passive Avoids
Escapes
0.2 zScore
Speed (cm/sec)
CS onset
US onset
sec
D
from response occurrence
Avoids
Escapes
Active Avoids
Active Avoid
Escape
E
Avoids
Escapes
F/Fo
Speed

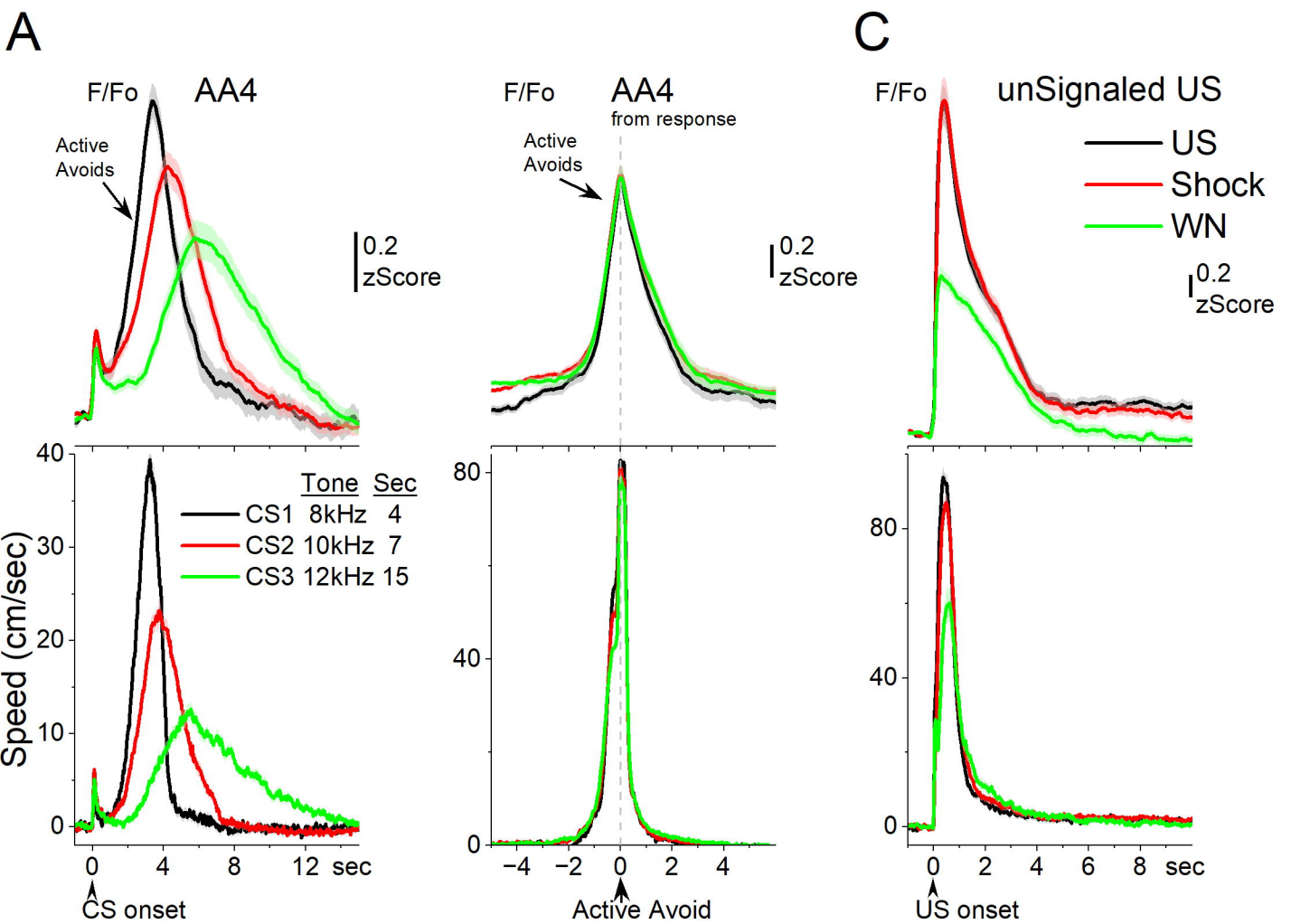
A
F/Fo
AA4
Active Avoids
0.2 zScore
Speed (cm/sec)
Tone Sec
CS1 8kHz 4
CS2 10kHz 7
CS3 12kHz 15
CS onset
sec
F/Fo
AA4
from response
Active Avoids
0.2 zScore
Active Avoid
C
F/Fo
unSignaled US
US
Shock
WN
0.2 zScore
US onset
sec

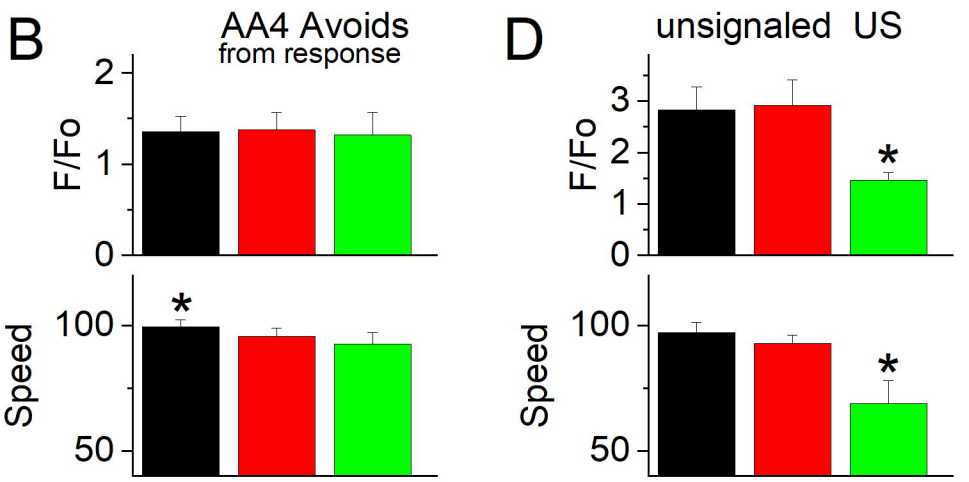
B
AA4 Avoids
from response
F/Fo
Speed
D
unsignaled US
F/Fo
Speed

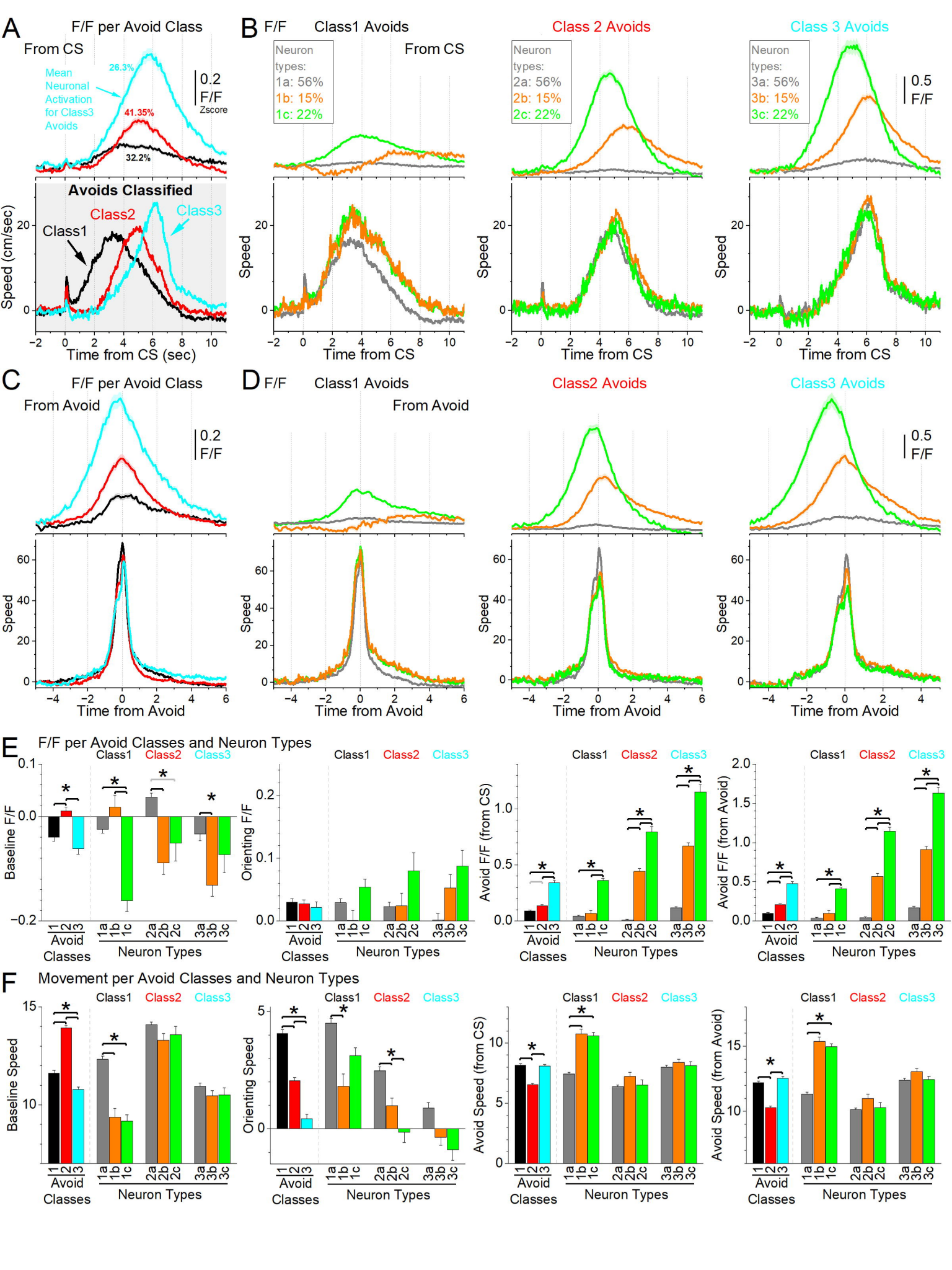
A
F/F per Avoid Class
From CS
Mean Neuronal Activation for Class3 Avoids
26.3%
41.35%
32.2%
0.2 F/F Zscore
Avoids Classified
Class1
Class2
Class3
Speed (cm/sec)
Time from CS (sec)
B
F/F
Class1 Avoids
Class 2 Avoids
Class 3 Avoids
From CS
Neuron types:
1a: 56%
1b: 15%
1c: 22%
2a: 56%
2b: 15%
2c: 22%
3a: 56%
3b: 15%
3c: 22%
0.5 F/F
Speed
Time from CS
C
F/F per Avoid Class
From Avoid
0.2 F/F
Speed
Time from Avoid
D
F/F
Class1 Avoids
Class2 Avoids
Class3 Avoids
From Avoid
0.5 F/F
Speed
Time from Avoid
E
F/F per Avoid Classes and Neuron Types
Class1
Class2
Class3
Baseline F/F
Orienting F/F
Avoid F/F (from CS)
Avoid F/F (from Avoid)
Avoid Classes
Neuron Types
F
Movement per Avoid Classes and Neuron Types
Baseline Speed
Orienting Speed
Avoid Speed (from CS)
Avoid Speed (from Avoid)

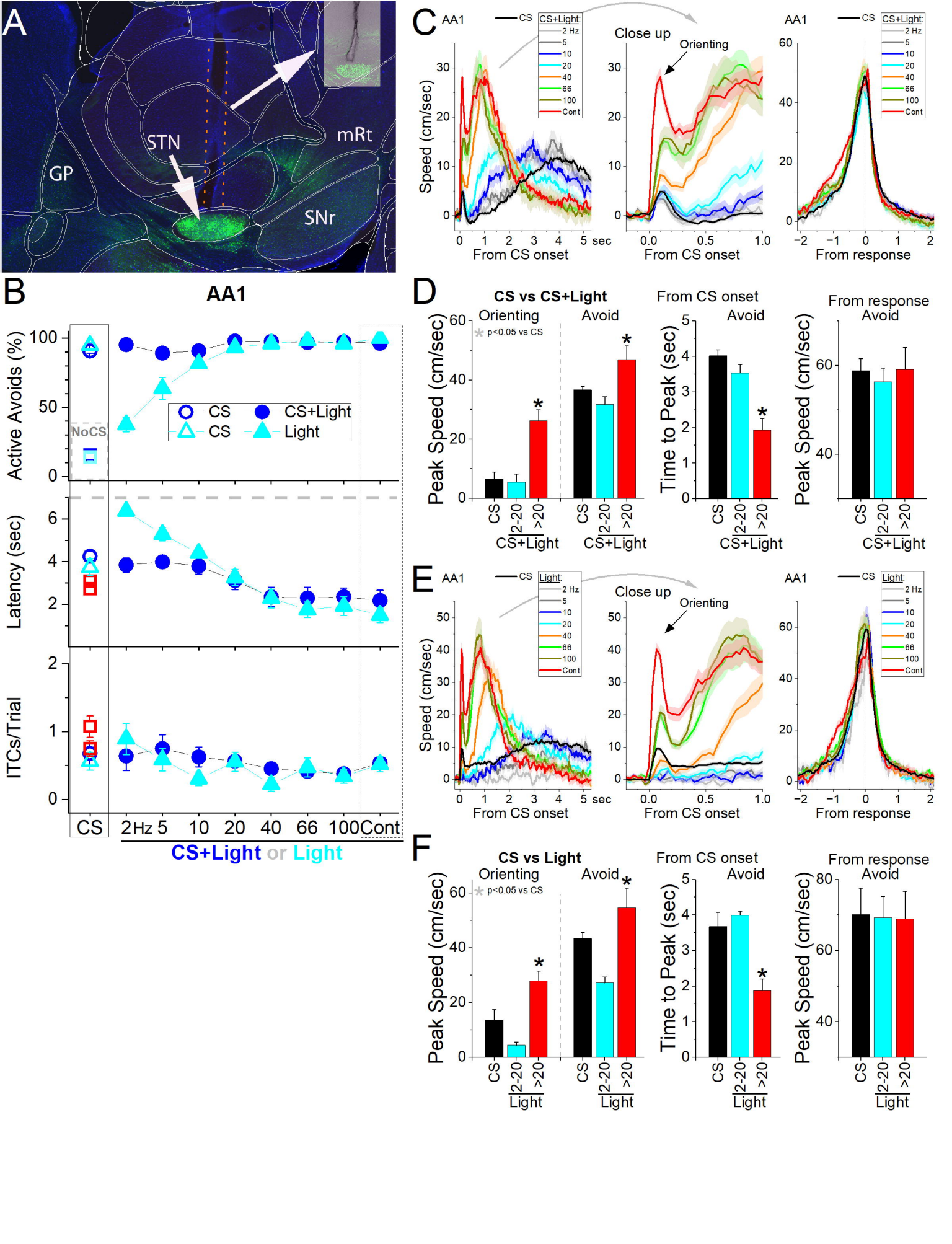
A
STN
GP
mRt
SNr
B
AA1
Active Avoids (%)
NoCS
CS
CS+Light
CS
Light
Latency (sec)
ITCs/Trial
CS
2Hz 5 10 20 40 66 100 Cont
CS+Light or Light
C
AA1
CS
CS+Light:
2 Hz
5
10
20
40
66
100
Cont
Close up
Orienting
Speed (cm/sec)
From CS onset
From response
D
CS vs CS+Light
Orienting
Avoid
p<0.05 vs CS
Peak Speed (cm/sec)
Time to Peak (sec)
CS
2-20
>20
CS+Light
E
Light:
F
CS vs Light
Light

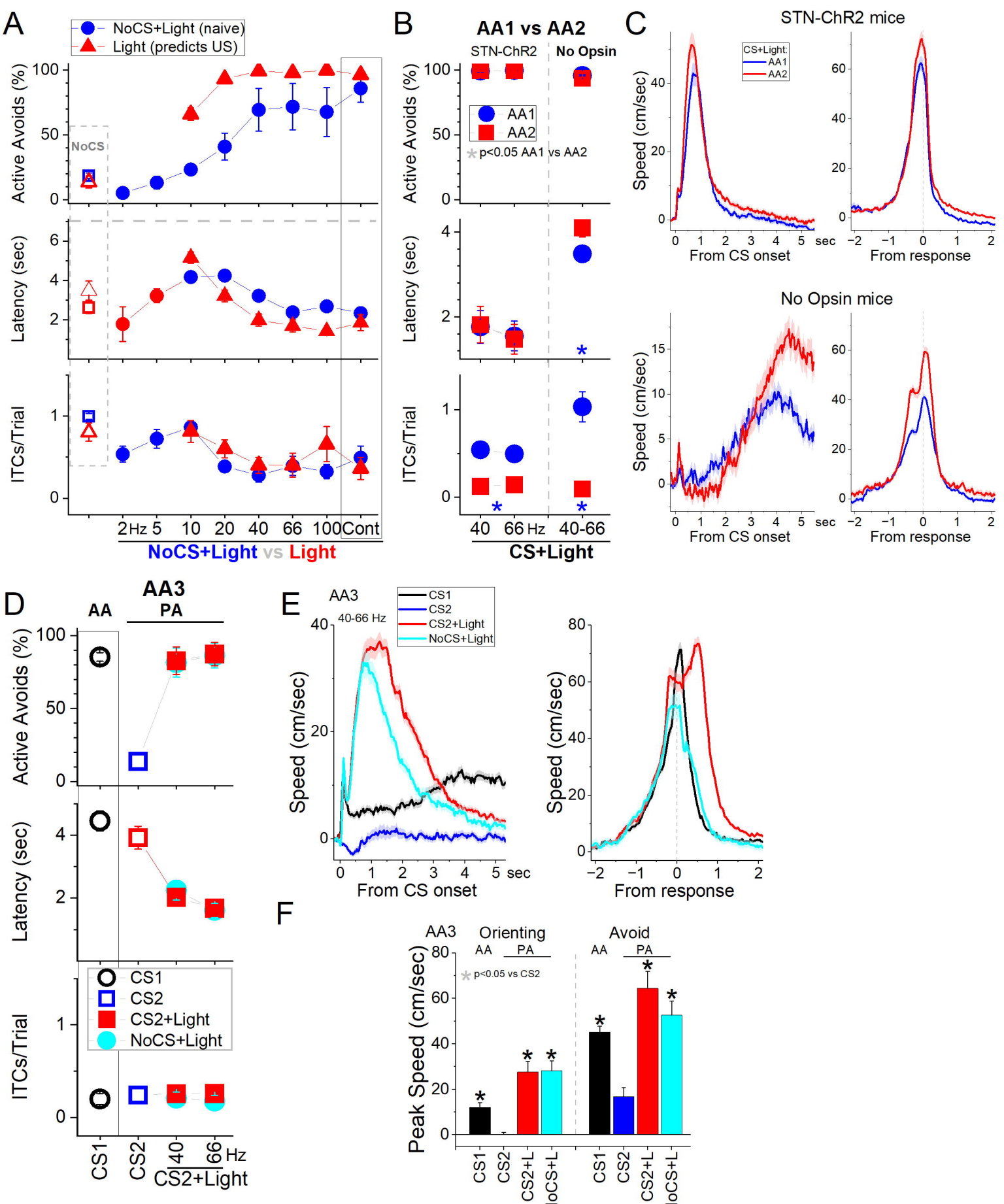
A
NoCS+Light (naive)
Light (predicts US)
Active Avoids (%)
NoCS
Latency (sec)
ITCs/Trial
2Hz 5 10 20 40 66 100Cont
NoCS+Light vs Light
B
AA1 vs AA2
STN-ChR2
No Opsin
AA1
AA2
* p<0.05 AA1 vs AA2
40 66 Hz 40-66
CS+Light
C
STN-ChR2 mice
CS+Light:
AA1
AA2
Speed (cm/sec)
From CS onset
From response
No Opsin mice
D
AA3
AA
PA
CS1
CS2
CS2+Light
NoCS+Light
CS2+Light
E
AA3
40-66 Hz
CS1
CS2
CS2+Light
NoCS+Light
F
AA3
Orienting
Avoid
* p<0.05 vs CS2
Peak Speed (cm/sec)
CS1 CS2 CS2+L NoCS+L

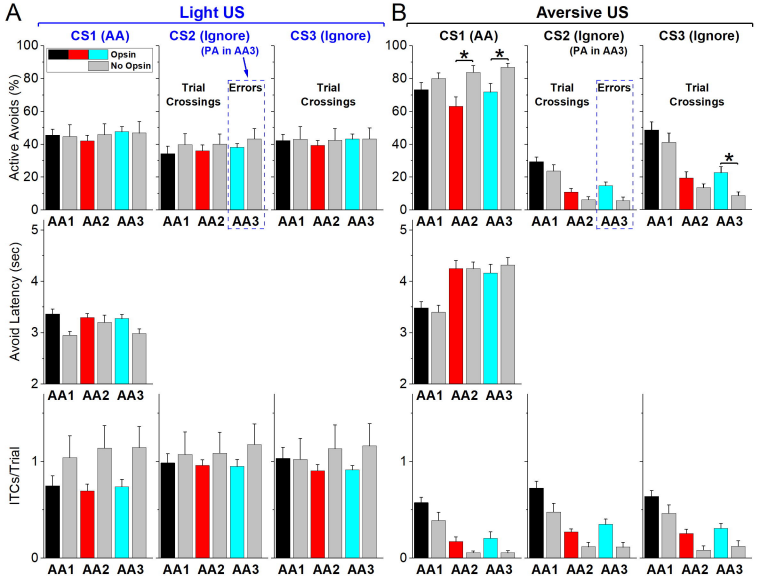
A
Light US
CS1 (AA)
CS2 (Ignore)
CS3 (Ignore)
Opsin
No Opsin
(PA in AA3)
Trial Crossings
Errors
Trial Crossings
Active Avoids (%)
Avoid Latency (sec)
ITCs/Trial
AA1 AA2 AA3
B
Aversive US
CS1 (AA)
CS2 (Ignore)
(PA in AA3)
CS3 (Ignore)
Trial Crossings
Errors
Trial Crossings
*

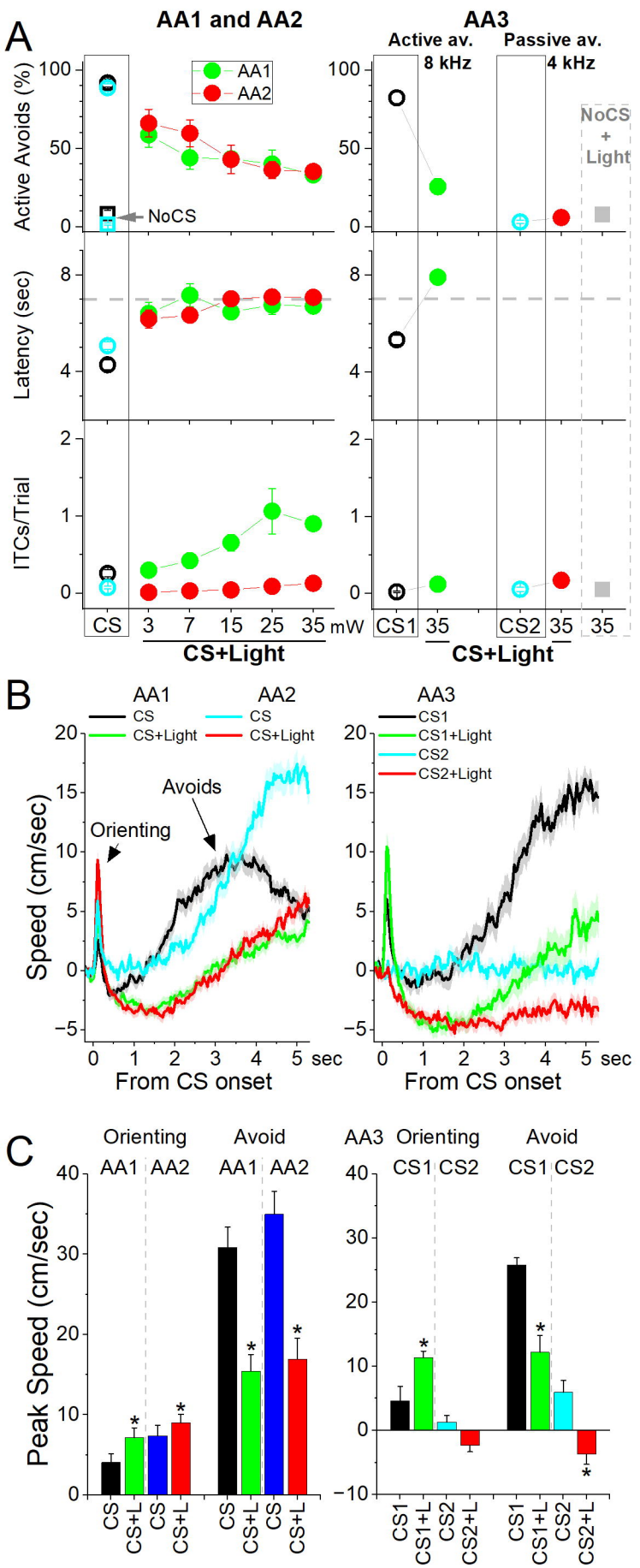
A
AA1 and AA2
AA3
Active av.
8 kHz
Passive av.
4 kHz
AA1
AA2
NoCS
NoCS
+
Light
Active Avoids (%)
Latency (sec)
ITCs/Trial
CS
3
7
15
25
35 mW
CS1
35
CS2
35
35
CS+Light
CS+Light
B
AA1
CS
CS+Light
AA2
CS
CS+Light
AA3
CS1
CS1+Light
CS2
CS2+Light
Avoids
Orienting
Speed (cm/sec)
From CS onset
sec
From CS onset
sec
C
Orienting
Avoid
AA1
AA2
AA1
AA2
AA3
Orienting
Avoid
CS1
CS2
CS1
CS2
Peak Speed (cm/sec)
CS
CS+L
CS
CS+L
CS
CS+L
CS
CS+L
CS1
CS1+L
CS2
CS2+L
CS1
CS1+L
CS2
CS2+L

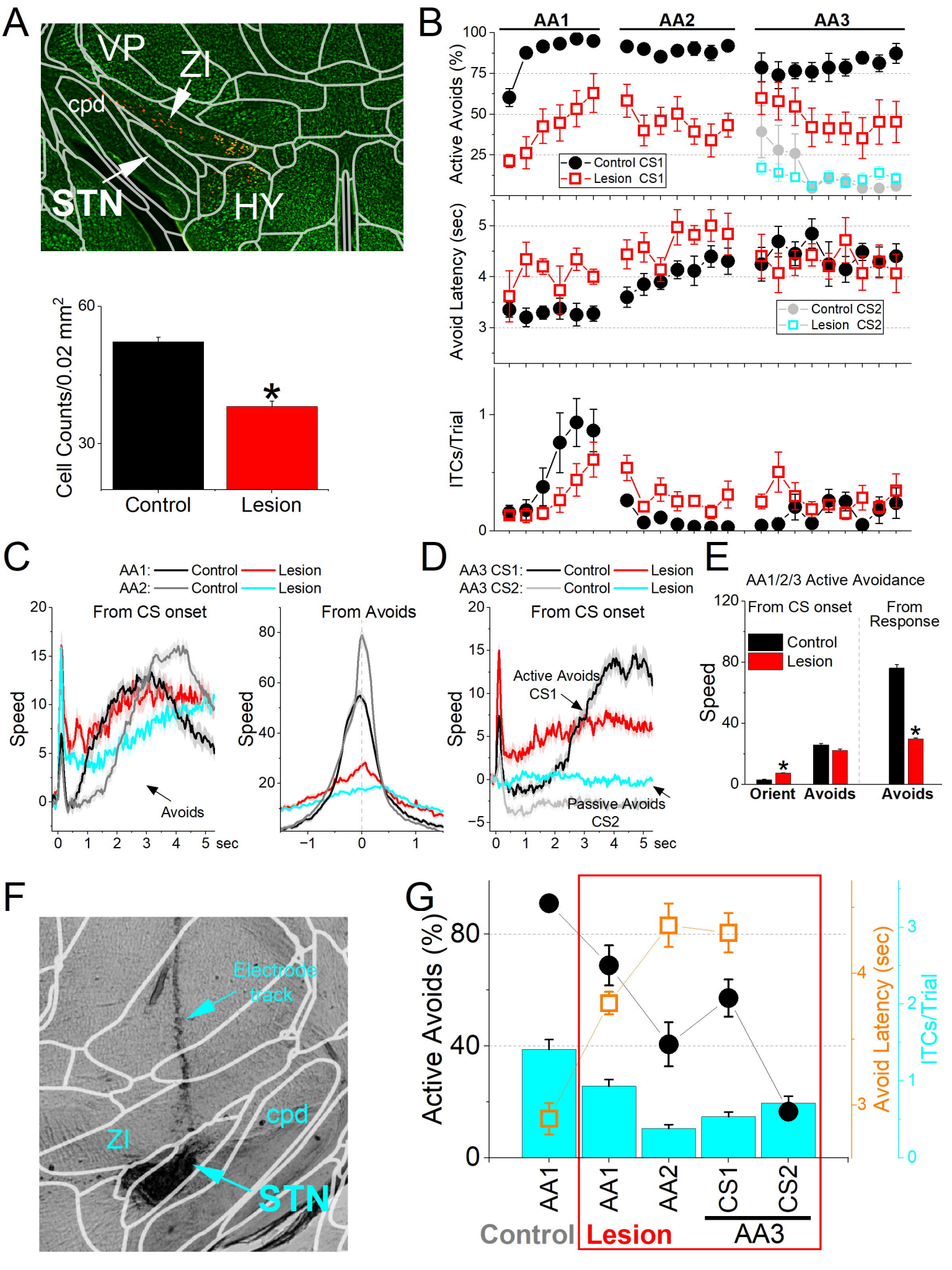
A
VP
ZI
cpd
STN
HY
Cell Counts/0.02 mm2
60
30
*
Control
Lesion
B
AA1
AA2
AA3
Active Avoids (%)
100
75
50
25
Control CS1
Lesion CS1
Avoid Latency (sec)
5
4
3
Control CS2
Lesion CS2
ITCs/Trial
1
0
C
AA1: Control Lesion
AA2: Control Lesion
From CS onset
From Avoids
Speed
20
15
10
5
0
Avoids
0 1 2 3 4 5 sec
80
60
40
20
−1 0 1
D
AA3 CS1: Control Lesion
AA3 CS2: Control Lesion
From CS onset
Active Avoids
CS1
Passive Avoids
CS2
−5
0 1 2 3 4 5 sec
E
AA1/2/3 Active Avoidance
From CS onset
From Response
Control
Lesion
120
80
40
0
Orient
Avoids
Avoids
F
Electrode
track
cpd
ZI
STN
G
Active Avoids (%)
80
40
0
Avoid Latency (sec)
4
3
ITCs/Trial
3
2
1
0
AA1
AA1
AA2
CS1
CS2
Control
Lesion
AA3

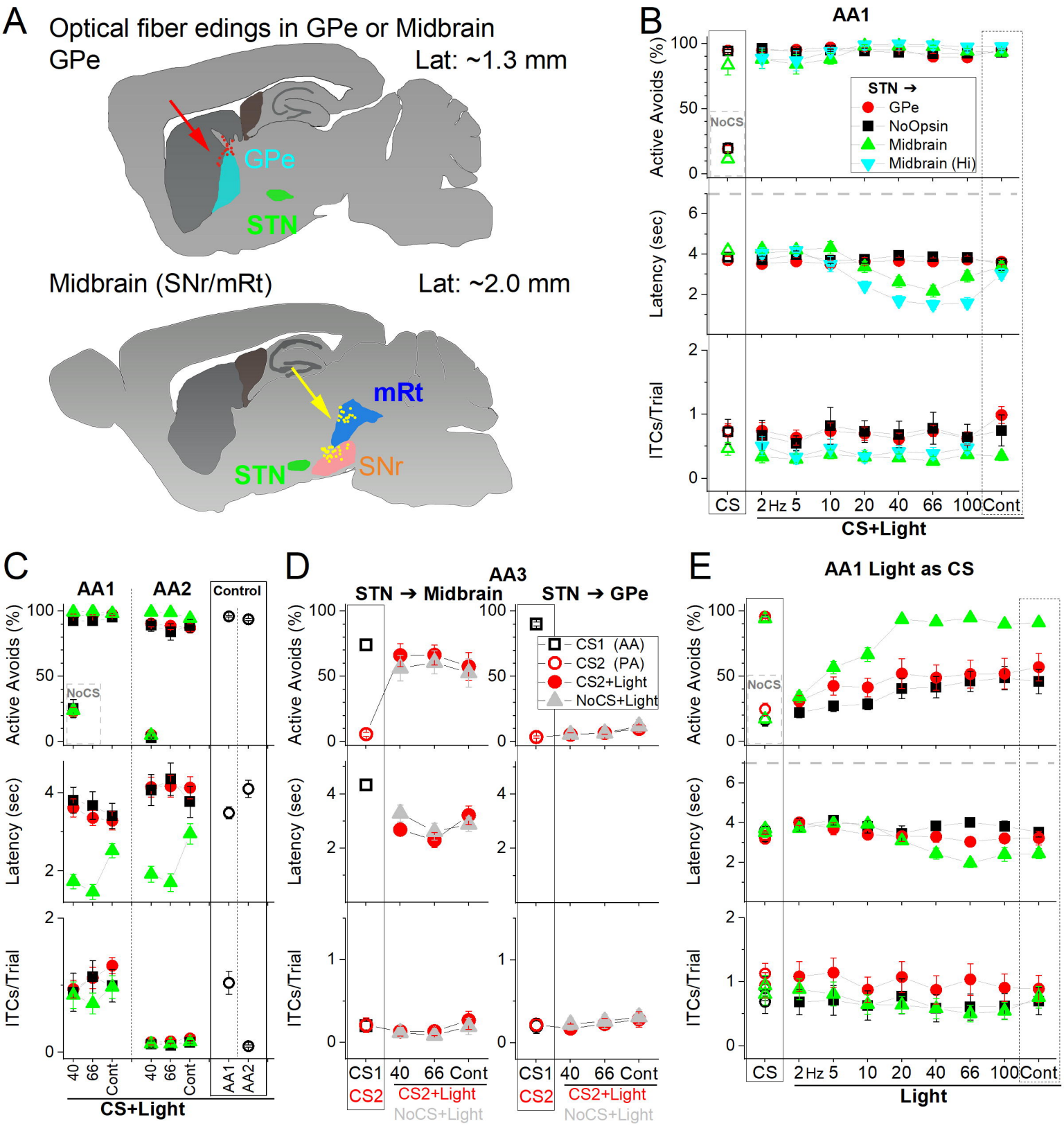
A
Optical fiber edings in GPe or Midbrain
GPe
Lat: ~1.3 mm
GPe
STN
Midbrain (SNr/mRt)
Lat: ~2.0 mm
mRt
STN
SNr
B
AA1
Active Avoids (%)
Latency (sec)
ITCs/Trial
NoCS
STN →
GPe
NoOpsin
Midbrain
Midbrain (Hi)
CS
2 Hz 5 10 20 40 66 100 Cont
CS+Light
C
AA1
AA2
Control
NoCS
40 66 Cont 40 66 Cont AA1 AA2
CS+Light
D
AA3
STN → Midbrain
STN → GPe
CS1 (AA)
CS2 (PA)
CS2+Light
NoCS+Light
CS1 40 66 Cont
CS2
CS2+Light
NoCS+Light
E
AA1 Light as CS
Light

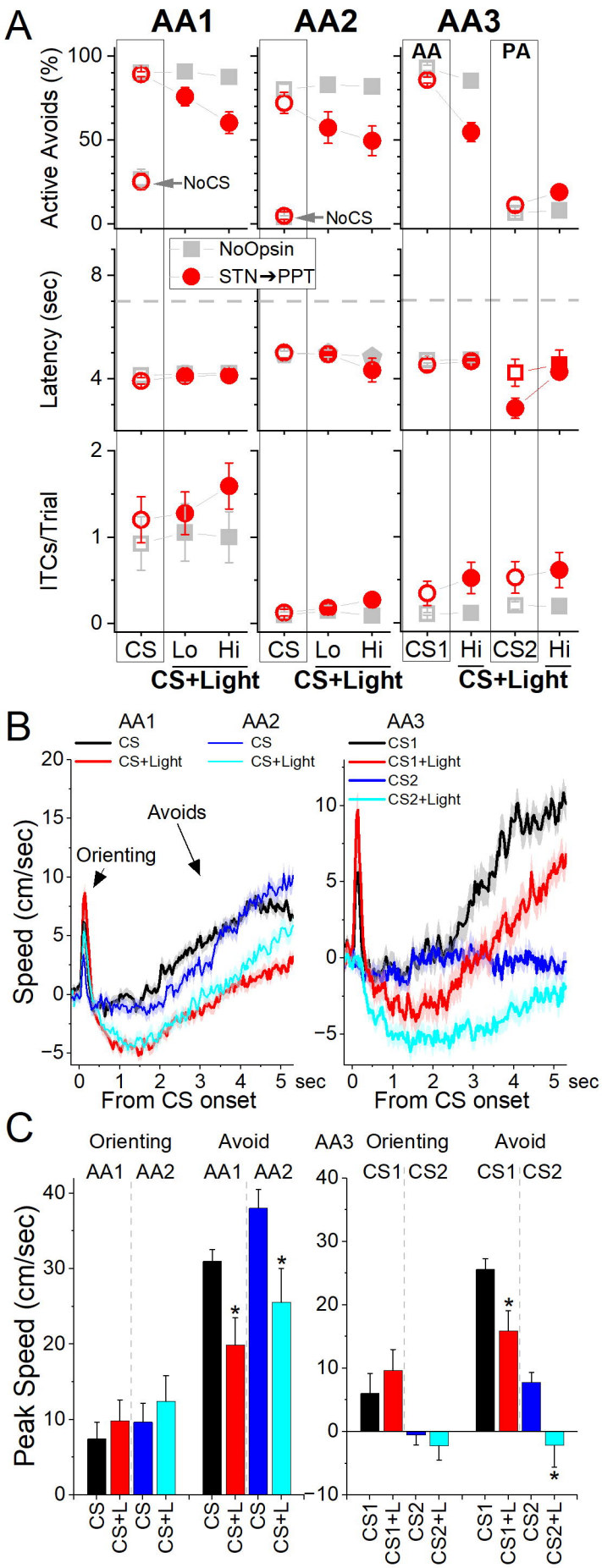
A
AA1
AA2
AA3
AA
PA
Active Avoids (%)
NoCS
NoOpsin
STN→PPT
Latency (sec)
ITCs/Trial
CS
Lo
Hi
CS1
CS2
CS+Light
B
Speed (cm/sec)
Orienting
Avoids
From CS onset
sec
CS+Light
CS1+Light
CS2+Light
C
Peak Speed (cm/sec)
Orienting
Avoid
CS+L
CS1+L
CS2+L